Estuarine, Coastal and Shelf Science 243 (2020) 106828

Contents lists available at ScienceDirect

Estuarine, Coastal and Shelf Science

journal homepage: http://www.elsevier.com/locate/ecss

Seasonal variations of net ecosystem (CO_2) exchange in the Indian tropical mangrove forest of Pichavaram

Palingamoorthy Gnanamoorthy [a,d,*], V. Selvam [a], Pramit Kumar Deb Burman [b,c], S. Chakraborty [b,c], A. Karipot [c], R. Nagarajan [a], R. Ramasubramanian [a], Qinghai Song [d], Yiping Zhang [d], John Grace [e]

[a] Coastal Systems Research, M. S. Swaminathan Research Foundation, Chennai, India
[b] Centre for Climate Change Research, Indian Institute of Tropical Meteorology, Ministry of Earth Sciences (MoEs), Pune, India
[c] Department of Atmospheric and Space Sciences, Savitribai Phule Pune University, Pune, India
[d] CAS, Key Laboratory of Tropical Forest Ecology, Xishuangbanna Tropical Botanical Garden, Chinese Academy of Sciences, Menglun, China
[e] School of GeoSciences, The University of Edinburgh, Edinburgh EH9 3FF, United Kingdom

ARTICLE INFO

Keywords:
Mangrove wetland
Carbon exchange
Net ecosystem productivity
Eddy covariance

ABSTRACT

Mangrove ecosystems play a crucial role in the global carbon cycle. However, the carbon fluxes in the mangrove ecosystems found in the Indian subcontinent are not well understood. Here, for the first time, we estimate the net ecosystem exchange (NEE) in a mangrove ecosystem at Pichavaram, southeast India, using the eddy covariance method for the period October 2017–September 2018. The half-hourly daytime NEE varied from −11.05 μmol m^{-2} s^{-1} in the winter months (January–March 2018) to −6.06 μmol m^{-2} s^{-1} during the summer (April 2018). The estimated annual evapotranspiration during the study period was 610 mm, whereas the precipitation was 653 mm (much dryer than the long-term average). The half-hourly NEE data were gap filled and partitioned to estimate the gross primary productivity (GPP) and ecosystem respiration (R_{eco}). The estimated annual GPP was 1466 gC m^{-2} and R_{eco} was 1283 gC m^{-2}. The mangrove forest appeared to be a modest sink of atmospheric CO_2, with an annual average net ecosystem productivity of 183 gC m^{-2}. However, in the summer months, it acted as a source. We observed that the mangrove CO_2 fluxes strongly responded to environmental factors such as temperature, rainfall, and salinity. However, it is noteworthy that the carbon sink capability may decline in the future due to rising temperatures, decreasing rainfall patterns, variation in salinity, and changes in tidal inundation patterns.

1. Introduction

Anthropogenic global warming is known to have caused major changes in temperature, precipitation, wind pattern, and sea level in the past one hundred years (IPCC et al., 2013). These climatic changes have also affected our life support systems, including forests, food, and water security (IPCC et al., 2013; Reichstein et al., 2013). To minimize the adverse effect of climate change, several countries pledged to maintain a cap on global temperature rise and keep the cap at about 1.5 °C under the Conference of Parties in Paris (COP21) initiative (Walsh et al., 2017). India, an important member-state of this consortium, has started several initiatives to reduce greenhouse gas emission and intensify the process of carbon sequestration. According to the Intended Nationally Determined Contribution (INDC), on the one hand, India has planned to enhance carbon sequestration annually by an equivalent of about 100 million tons of CO_2 through better management practices and by increasing the tree cover by using forest lands under the initiatives of the Green India Mission (GIM) programme (Ravindranath and Murthy, 2010). On the other hand, to better understand the carbon sequestration process in Indian forests and coastal ecosystems, an enhancement of our scientific understanding through a well-managed observational network, which would include eddy covariance (EC) measurements of CO_2 fluxes (Sundareshwar et al., 2007), was proposed.

The amount of carbon stored in a forest and its potential to exchange the carbon with the atmosphere largely depend on the nature of the forest. For example, global tropical forests are estimated to store about 45% of terrestrial carbon (Bonan, 2008; Beer et al., 2010), and hence they are believed to play a significant role in the carbon cycle. Mangrove

* Corresponding author. Coastal Systems Research, M. S. Swaminathan Research Foundation, Chennai, India.
E-mail addresses: pg.moorthy87@gmail.com, gnanamoorthy@xtbg.ac.cn (P. Gnanamoorthy).

https://doi.org/10.1016/j.ecss.2020.106828
Received 27 March 2019; Received in revised form 17 April 2020; Accepted 6 May 2020
Available online 6 June 2020

forests, in contrast, occupy only a small fraction, about 0.5%, of global coastal areas (Alongi, 2014). They are considered as valued ecosystems due to the role they play in supporting fisheries, protecting the shoreline, and providing a significant source of livelihood to coastal communities; they also play a very important role in mitigating the effects of climate change (Barr et al., 2012; Jennerjahn et al., 2017; Dai et al., 2018). Besides, mangrove wetlands have high rates of primary productivity and low decomposition processes (Ward et al., 2006). Globally, mangrove forests are thought to sequester about 218 ± 72 Tg C y^{-1} (Bouillon et al., 2008). Consequently, understanding the dynamics of water and carbon exchange in the mangrove forests and its responses to biotic and abiotic factors is of great importance, not only for understanding the carbon balance but also for the future protection and better management of these ecologically vulnerable ecosystems.

The EC method is one of the best practices for the estimation of trace gas and energy fluxes over natural ecosystems (Baldocchi, 2003; Burba, 2013). Numerous studies have been undertaken globally using the EC technique in different types of terrestrial ecosystems (Verma et al., 1986; Grace et al., 1995; Baldocchi, 1997; Law et al., 2000; Aubinet et al., 2001; Hanson et al., 2004; Tan et al., 2011; Fei et al., 2018), including mangroves (Barr et al., 2010, 2013a; 2014; Li et al., 2014; Leopold et al., 2016; Cui et al., 2018; Liu and Lai, 2019). Studies from across the globe in mangroves having semi-arid to humid climatic conditions have been reported by many investigators. For example, Leopold et al. (2016) estimated the annual net ecosystem productivity (NEP) of the semi-arid dwarf mangrove of New Caledonia to be much lower than that of mangroves in humid climates. The NEP value reported from Everglades National Park in western Florida, United States, was 1170 gC m^{-2} yr^{-1}, which was unusually high and attributed to year-round productivity and low ecosystem respiration (R_{eco}) in this humid mangrove ecosystem (Barr et al., 2010). Liu and Lai (2019) recently estimated the interannual carbon uptake rates to be 890 and 758 gC m^{-2} in the subtropical mangrove wetland of the northwestern region of Hong Kong, China. They found that temperature and salinity are the key controlling factors of mangrove carbon sink.

In India, several investigators have reported trace gas exchanges in different forest ecosystems, such as mixed deciduous forests in the central part of the country (Jha et al., 2013), subtropical deciduous Sal forests at Barkot, Uttarakhand (Watham et al., 2017), mixed plantation and natural forests at Haldwani, Uttarakhand (Watham et al., 2014), the agricultural site dominated by wheat crop at Meerut (Patel et al., 2011) and sesame crop at Barkachha (Deb Burman et al., 2020a), both in Uttar Pradesh, semievergreen forests in Assam, northeast India (Sarma et al., 2018; Deb Burman et al., 2019), and high-altitude Himalayan forests in eastern India (Chatterjee et al., 2018). However, the mangrove system is less studied. To our knowledge, only the mangrove forests of the Sundarbans in the Gangetic delta have been investigated using the EC flux method (Mukhopadhyay et al., 2000; Ganguly et al., 2008; Chanda et al., 2013; Jha et al., 2014; Rodda et al., 2016). These studies indicate that the Sundarbans mangrove ecosystem acts as a sink for CO_2 during the daytime with varying magnitude of 5.5–51.1 gC m^{-2} d^{-1} (Chanda et al., 2013; Rodda et al., 2016).

A micrometeorological observational network based on the EC technique, named MetFlux India (Deb Burman et al., 2017, 2020b; Chatterjee et al., 2018; Sarma et al., 2018), was initiated by the Ministry of Earth Sciences, Government of India, and executed by the Indian Institute of Tropical Meteorology, Pune, Maharashtra. Under this platform, the present study was undertaken by the M. S. Swaminathan Research Foundation, Chennai, Tamil Nadu, for the long-term monitoring of carbon, water, and energy fluxes over a mangrove ecosystem at Pichavaram in Tamil Nadu. Here, we report our initial observation of CO_2 flux measurement for a period of 1 year (October 2017–September 2018) from this station.

The carbon sequestration process in the coastal habitat mainly depends on local climatic conditions, tidal inundation patterns, and water salinity (Barr et al., 2010; Li et al., 2014; Leopold et al., 2016; Liu and Lai, 2019). The Pichavaram mangrove wetland belongs to the tropical wet and dry region, with a lower mean annual rainfall when compared with the mangrove ecosystems of China and the United States (Barr et al., 2010; Liu and Lai, 2019). The spatial distribution pattern of Pichavaram mangrove flora shows two different zones: the *Rhizophora* zone and the *Avicennia* zone (Selvam et al., 2002). The *Rhizophora* zone is characterized by dense and highly productive evergreen trees occurring in the narrow strip along the tidal creeks in the lower intertidal area. The *Avicennia* zone species grow in the higher salinity zone having lower tidal inundation due to the elevation, which directly affects the productivity of the plants (Santini et al., 2015; Leopold et al., 2016). The recent EC-based results also show the New Caledonia dwarf *Avicennia marina* to have lower net productivity than the other mangrove ecosystems (Leopold et al., 2016). The Pichavaram mangrove wetland is also dominated by *A. marina* (74%) species. These are generally short in height, and their carbon sequestration capacity is projected to be low. The main objective of our study is to investigate the carbon sequestration potential of this ecosystem by measuring the net ecosystem exchange (NEE) and thereby quantify the gross primary productivity (GPP) and respiration components of the carbon exchange with the atmosphere. We hypothesize that mangrove NEE would show substantial seasonal variability depending on wet than the dry seasons. Another important hypothesis is that air temperature, photosynthetically active radiation (PAR), vapor pressure deficit (VPD), annual rainfall, and water salinity are critical environmental regulators for the NEP of the Pichavaram mangrove ecosystem.

2. Materials and methods

2.1. Study site

The present study was carried out in the Pichavaram tropical mangrove wetland (lat. 11°20′N; long. 79°55′E) located between the Vellar and Coleroon estuaries of the Cauvery delta on the southeastern coast of peninsular India (Fig. 1). The land use and land cover patterns show that in the dense mangrove forests occupy an area of 813 ha, sparse mangrove vegetation about 68 ha, marshy vegetation about 664 ha, and mudflats about 340 ha. It consists of about 51 small islands covered by mangrove vegetation (Selvam et al., 2002). There are 12 species of true mangroves present in the Pichavaram mangrove wetland. The average leaf area index (LAI) in the *Rhizophora* zone is greater than that in the *Avicennia* zone, and the values range between 2 and 4 m^2 m^{-2}, respectively. The height of the mangroves ranges between 3 and 7.5 m (Selvam et al., 2002).

Unlike most of the country, the southeastern part of peninsular India receives maximum rainfall during the northeast monsoon season (NEM) (October–December) (IMD, 1973; Balachandran et al., 2006; Rajeevan et al., 2012). Therefore, the seasonality in Pichavaram is defined as follows: winter or post-monsoon (January–March), summer (April–June), pre-monsoon (July–September), and northeast monsoon (October–December) (http://www.imdchennai.gov.in/northeast_monsoon.htm) (Kathiresan, 2000). As per the Köppen climate classification, Pichavaram is subhumid with hot (atmospheric temperature >30 °C) summer and an average rainfall of about 1310 mm per annum (Gnanappazham and Selvam, 2014). The depth of water in the mangrove is shallow and varies approximately between 0.3 and 3.0 m (Selvam, 2003). The semidiurnal tidal patterns occur with slight inequality, and the overall spring and neap tidal ranges in the site are 0.82–0.34 m. In the EC flux tower neighborhood, the maximum tidal variation during the northeast monsoon is 50 cm, while the minimum variation is about 20 cm. Even in the summer months, the variation is between 25 and 38 cm (Selvam et al., 2002).

2.2. Eddy covariance flux tower and sensor setup

A 10 m tall EC flux tower was established in the Pichavaram

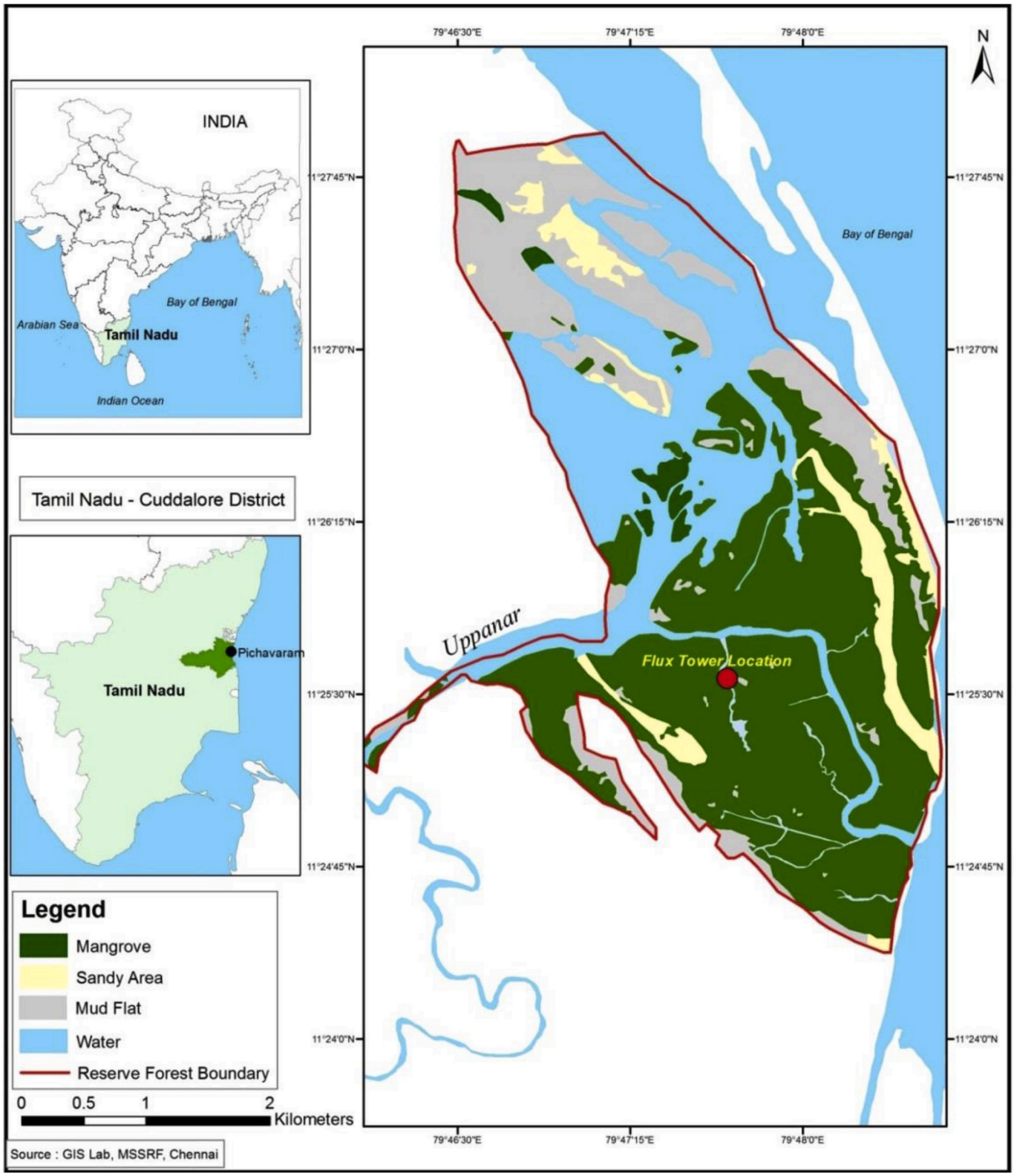

Fig. 1. Geographic location of the study site. The upper left panel shows the map of India. The middle panel shows the state of Tamil Nadu, the dark green shading represents Cuddalore district, and the black dot indicates Pichavaram. A zoomed-in image of the study area is shown in the right panel, where the red dot indicates the eddy covariance flux tower location. (For interpretation of the references to color in this figure legend, the reader is referred to the Web version of this article.)

mangrove to measure the CO_2, H_2O, and energy fluxes (Fig. 2). The tower is surrounded by a continuous dense mangrove patch with dominant species, namely, *A. marina* and *Rhizophora* spp, having a mean canopy height of about 3 m. It is fueled by three solar power systems (one 24 v and two 12 v each) with rechargeable batteries (500 AH). Micrometeorological and trace gas (CO_2 and H_2O) measurements were made at 10 m on the tower, 6.5 m above the top of the canopy. A three-dimensional (3D) sonic anemometer (Wind Master Pro, Gill Instruments,

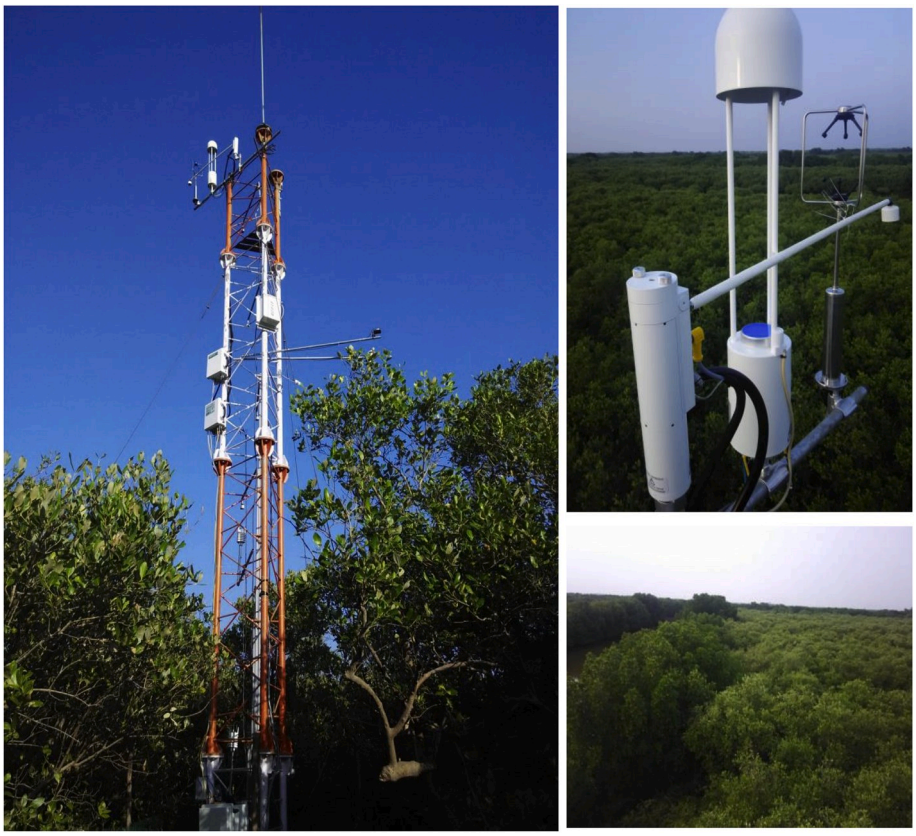

Fig. 2. Eddy covariance (EC) flux tower (left) in the dense area of Pichavaram mangrove forest. The CO_2/H_2O infrared gas analyzer system sensor and sonic anemometer and a part of the mangrove vegetation are shown in the right column upper and lower figures, respectively.

United Kingdom) was installed to measure the high-frequency wind velocity components and sonic temperature (T_s). The closed-path infrared gas analyzer system (IRGA) LI-7200 (LI-COR, Lincoln, Nebraska, United States) was installed to measure the concentrations of carbon dioxide and water vapor. The raw measurements from the sonic anemometer and IRGA were recorded using an analyzer interface unit, LI-7550 (LI-COR, Lincoln, Nebraska, United States), at a frequency of 10 Hz. The additional meteorological variables were being measured above the canopy at 10 s intervals and averaged over 1 min and 30 min; they were logged in a CR3000 (Campbell Scientific Inc., Logan, Utah, United States) data logger. These measurements included net radiation (NR01, Hukseflux) and incoming photosynthetic active radiation (SQ-100 and -300 series, Apogee instruments) at the height of 6 m. Other meteorological measurements included air temperature, relative humidity, wind speed, wind direction, and precipitation at heights of 2 m, 6 m, and 10 m (Vaisala weather transmitter WXT520, Finland). In addition, soil heat flux was also measured at two depths (2.5 and 5 cm) (HFP01SC-20, Hukseflux). Around the EC flux tower, three sampling sites were fixed to monitor (*in situ*) the weekly water salinity using a water quality monitoring system (Hydrolab Quanta Multi-Probe Meter).

2.3. Eddy covariance flux measurements

The EC method is known to be a reliable technique of measuring the net carbon exchange between the mangrove ecosystem and atmosphere (Barr et al., 2010; Rodda et al., 2016).

The following equation is used to calculate CO_2 flux, as defined in Baldocchi (2003):

$$\text{NEE} = \overline{\rho_\alpha}.\omega' c', \quad (1)$$

where ρα is the air density, ω′ is the vertical wind speed, and c′ is CO_2 concentration fluctuations from the respective means. The overbar in the equation indicates time averaging. Negative CO_2 flux denotes carbon uptake by the vegetation, and positive flux denotes CO_2 release into the atmosphere. Half-hourly data from October 2017 to September 2018 were used in our analysis.

2.4. Primary data processing

The raw EC flux data were processed from October 2017 to September 2018 using EddyPro processing software (version 6.1.0, LI-COR, Lincoln, Nebraska, United States) to calculate the 30-min averaged CO_2, H_2O, and energy fluxes. Triple-coordinate rotation was applied to eliminate errors due to sensor tilt (Baldocchi et al., 2000; Wilczak et al., 2001); the site has more or less homogenous terrain. WPL correction was applied to correct CO_2 and H_2O fluxes for air-density variations from the transfer of heat and water vapor (Webb et al., 1980). The data with larger spikes due to instrument error were removed during the processing of each data file (Sabbatini et al., 2018).

2.5. Secondary data processing

The secondary data processing methodology used is similar to the proposed corrections by Thomas et al. (2011). Data recorded during heavy rain conditions were eliminated (Yu et al., 2006). Low turbulence at night may cause the night-time fluxes to be underestimated (Goulden et al., 1996; Baldocchi, 2003; Lei and Yang, 2010). Accordingly, if friction velocity (u^*) was less than 0.13 ms^{-1}, as determined by an average value test (AVT) (Zhu et al., 2006), then these data were rejected. Night-time negative CO_2 fluxes, if any, were rejected if PAR was less than 5 μmol $m^{-2}s^{-1}$ (Wang et al., 2013). After this filtering technique, approximately 93% of the CO_2 fluxes remained. In the present study, the annual u^* threshold was evaluated using an online tool (https://www.bgc-jena.mpg.de/bgi/index.php/Services/REddyProcWe

bUStarFiltering) as 0.21 ms^{-1}; a total of 7% of the data was marked as the gap from the available dataset. Filtered data were then gap-filled using the online EC processing tool of the Department of Biogeochemical Integration at the Max Planck Institute for Biogeochemistry (http://www.bgc-jena.mpg.de/~MDIwork/eddyproc/). Further, the gap-filled data were partitioned into GPP and R_{eco}.

2.6. Flux portioning

The NEE was partitioned into two components, GPP and R_{eco} (Kolari et al., 2004; Reichstein et al., 2005):

$$NEE = R_{eco} - GPP. \quad (2)$$

The GPP and R_{eco} were calculated by an online EC processing tool, as mentioned earlier, a procedure often followed by the FLUXNET and EUROFLUX communities (Wutzler et al., 2018).

3. Results

3.1. Meteorological variations

Fig. 3(a–d) shows the half-hourly records of meteorological parameters on a monthly scale. From October 2017 to September 2018, the

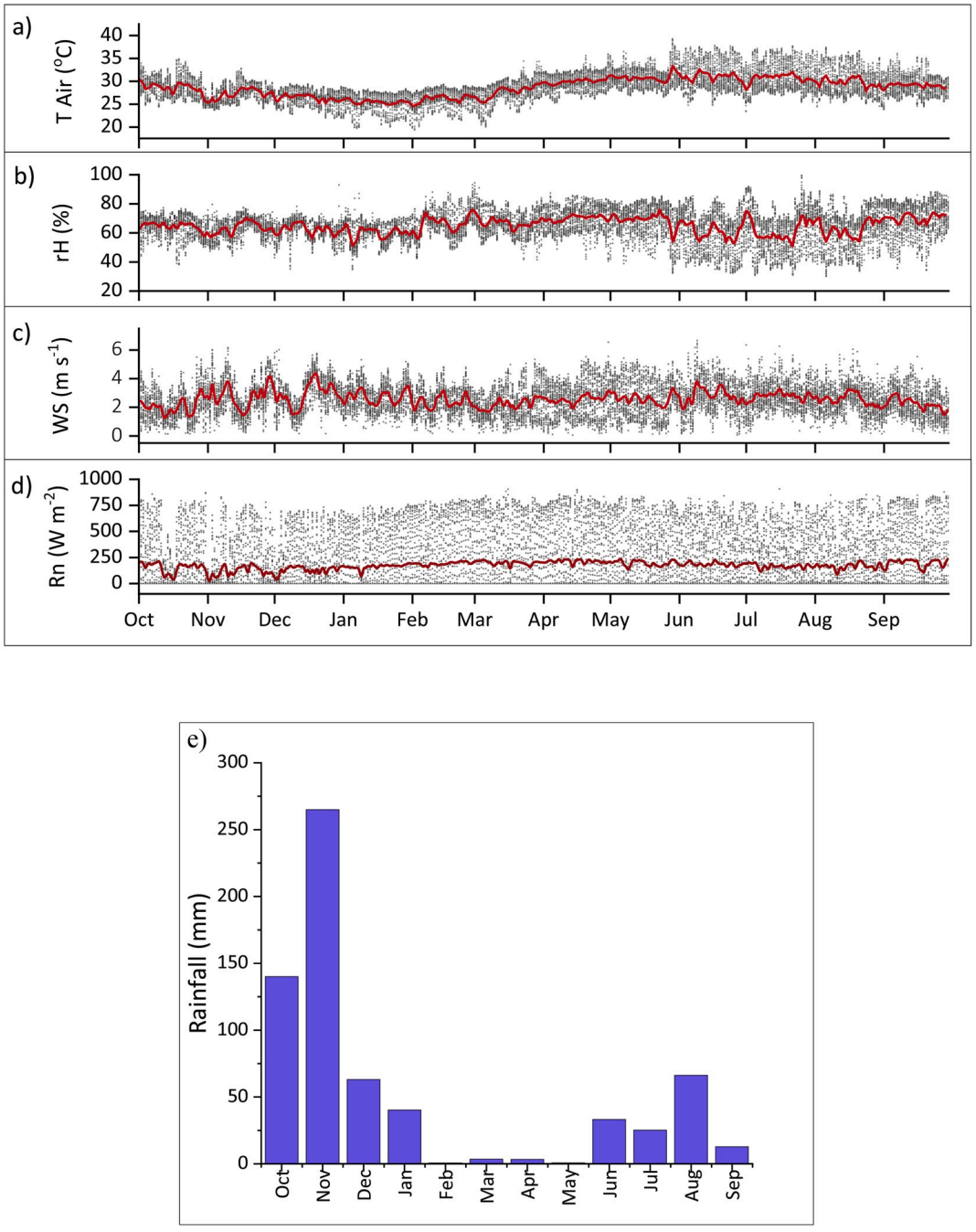

Fig. 3. Continuous measurement of climatological data for each month of the year (half-hourly data). (a) Air temperature (TAir) measured at 10 m above the ground; (b) relative humidity (rH) variations in monthly scale; (c) monthly variations of wind speed (WS); (d) solar net radiation (Rn) variations; and (e) monthly total rainfall recorded in the study area from October 2017 to September 2018. Red lines in panels (a–d) show the daily averages. (For interpretation of the references to color in this figure legend, the reader is referred to the Web version of this article.)

lowest air temperature (22 °C) was observed in January (winter or post-monsoon), and the peak temperature (35.5 °C) was recorded in June (summer). Seasonal variations of air temperature in the Pichavaram mangroves indicated that May–June was the hottest season with a monthly average temperature of 30.9 °C, whereas the lowest temperature of 25.8 °C was observed during January–February (Fig. 3a). The relative humidity ranged from 42% to 79%, the average is 67% (Fig. 3b). The monthly wind speed ranged from 1 ms^{-1} (April) to 4.31 ms^{-1} (May) (Fig. 3c). The highest value of the net radiation was about 700 Wm^{-2} observed in March and April (Fig. 3d). The total rainfall during the entire study period was 653.3 mm, with nearly 72% of the total annual rainfall during the northeast monsoon (October–December). The site recorded the highest rainfall of 265 mm in November; this was due to the effect of the northeast monsoon (Fig. 3e).

3.2. Determination of the CO_2 fluxes

The wind rose diagram shows the prevailing wind direction and speed, and the footprint analysis was done to determine the EC flux source area (Fig. 4a and b) (Schmid, 2002). The prevailing wind directions at the study site were west-north-west and west-south-east, and the wind speed mainly stayed in the range of 0.8–4.4 ms^{-1} during the entire study period (Fig. 4a). The footprint or fetch (90%) of the study site ranged from 208 to 335 m, with an average value of 206 m in the flux tower (Fig. 4b).

Fig. 5 shows the gap-filled half-hourly monthly variations of NEE over the period of October 2017–September 2018. We followed the standard micrometeorological convention for our analysis. CO_2 uptake due to photosynthesis is considered as negative, while the positive flux indicates CO_2 loss by respiration. The half-hourly NEE ranged from −17.34 μmol m^{-2} s^{-1} (December 23, 2017) to 9.9 μmol m^{-2} s^{-1} (October 25, 2017) (Fig. 5). The seasonal variation of diurnal patterns of CO_2 flux is presented in Fig. 6(a–d). During the northeast monsoon season (October–December), the CO_2 flux varied from −8.50 μmol m^{-2} s^{-1} in the daytime to 3.63 μmol m^{-2} s^{-1} in the night-time. In contrast, in the winter or post-monsoon season (January–March), the fluxes varied from −11.05 μmol m^{-2} s^{-1} in the daytime to 4.05 μmol m^{-2} s^{-1} in the night-time. During the summer season, CO_2 fluxes were quite low compared to other seasons; they ranged from −6.06 μmol m^{-2} s^{-1} in the daytime to 4.27 μmol m^{-2} s^{-1} in the night-time. During the pre-monsoon season, the NEE varied from −9.21 μmol m^{-2} s^{-1} to 5.11 μmol m^{-2} s^{-1}. The mean daytime flux contributed by photosynthesis was −5 μmol m^{-2} s^{-1}, whereas the mean night-time flux due to respiration was 3.31 μmol m^{-2} s^{-1} (Fig. 7a and b).

3.3. Carbon source and sink

The minimum GPP and R_{eco} values of 0.21 and 2.42 gC m^{-2} d^{-1}, respectively, were observed in the month of November while the maximum values of 6.32 and 4.96 gC m^{-2} d^{-1}, respectively, were observed in September (Fig. 8a and b). GPP, R_{eco}, and NEP values were found to vary considerably by season (Table 1). Overall, the GPP values were higher than the R_{eco} values, but during the summer months of June and July, the R_{eco} exceeded the GPP, making the ecosystem a carbon source; for the rest of the year, it acted as a carbon sink. The NEP values were calculated as the incoming GPP minus the R_{eco} (NEP = GPP - R_{eco}). Fig. 8c shows the half-hourly NEP values ranging from 2.49 gC m^{-2} d^{-1} in January to the lowest negative value of −2.34 gC m^{-2} d^{-1} in November. During June and July, the ecosystem acted as a net carbon source with the monthly averaged values being −0.54 and −0.26 gC m^{-2} d^{-1}, respectively. The overall estimates of GPP, R_{eco}, and NEP during our study period (October 2017–September 2018) were 1466, 1283, and 183 gC m^{-2} y^{-1}, respectively. The study shows that the Pichavaram mangrove ecosystem served as a carbon sink, and the average annual sum of the NEP was 1.83 tC ha^{-1}.

3.4. Seasonal net ecosystem exchange responses to photosynthetically active radiation

The rectangular hyperbolic least-square fits of PAR with daytime half-hourly NEE during different seasons were investigated using the Michaelis-Menten equation (Falge et al., 2001) given here and shown in Fig. 9(a–d).

$$NEE = \frac{\alpha * PAR * Pmax}{\alpha * PAR * Pmax} - R_{eco} \quad (3)$$

where α represents the apparent quantum yield (μmol CO_2 μmol photon^{-1}), PAR is photosynthetically active radiation (μmol m^{-2} s^{-1}), Pmax represents the maximum photosynthetic rate, and R_{eco} is the daytime ecosystem respiration (μmol CO_2 m^{-2} s^{-1}).

The carbon sequestration ability increased with PAR irrespective of the season. However, the ecosystem showed higher apparent quantum yield (−0.025 μmol CO_2 μmol photon^{-1}) in the winter or post-monsoon season (January–March; R^2 = 0.82) (Fig. 9b) than in the northeast monsoon season (October–December; R^2 = 0.78) (Fig. 9a). This is a strong indication that the most of the carbon sequestration took place during the post-monsoon season. A high level of scattering was observed between PAR and NEE during the summer months (April–June). The averaged CO_2 flux was about −3.72 μmol m^{-2} s^{-1} and noon

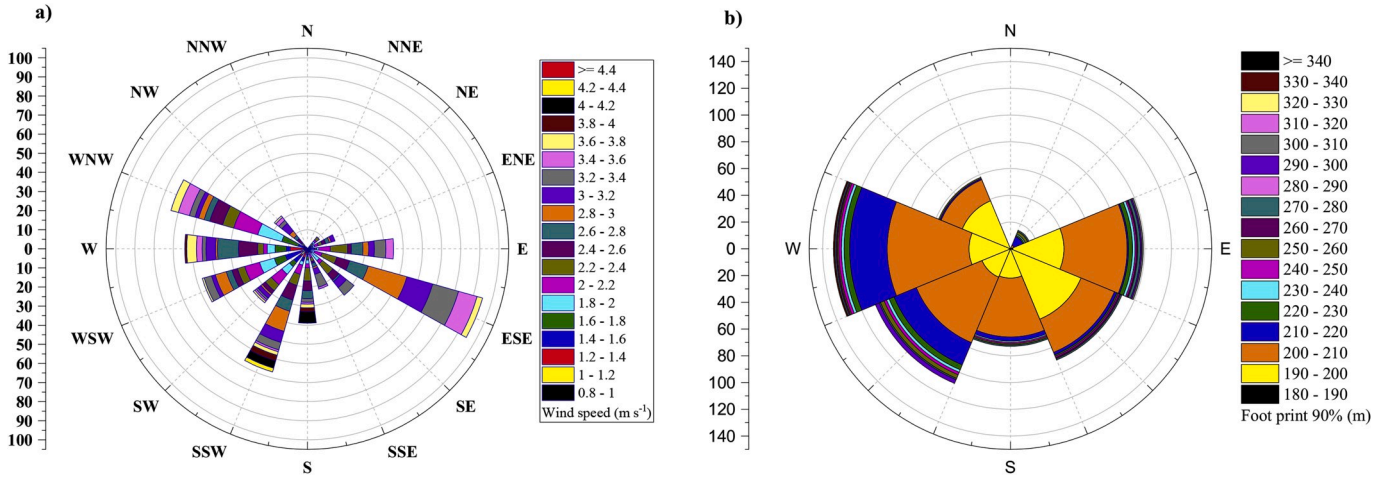

Fig. 4. Wind rose and footprint of the eddy covariance system in the Pichavaram mangrove ecosystem of the study site. (a) Wind rose diagram showing the wind speed and direction at the study site. The stripes show the direction, while its color represents the wind speed. (b) Footprint (m) calculated for the study site ranged from 208 to 335 m. (For interpretation of the references to color in this figure legend, the reader is referred to the Web version of this article.)

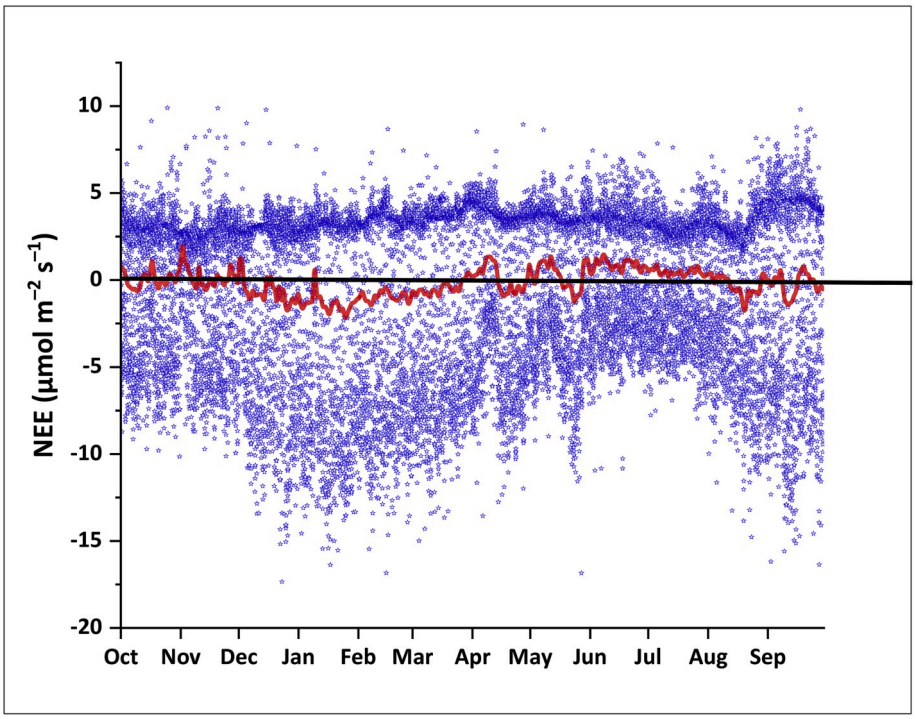

Fig. 5. Half-hourly CO_2 flux variations on a monthly time scale from October 2017 to September 2018. Red lines in panel show the daily averages. (For interpretation of the references to color in this figure legend, the reader is referred to the Web version of this article.)

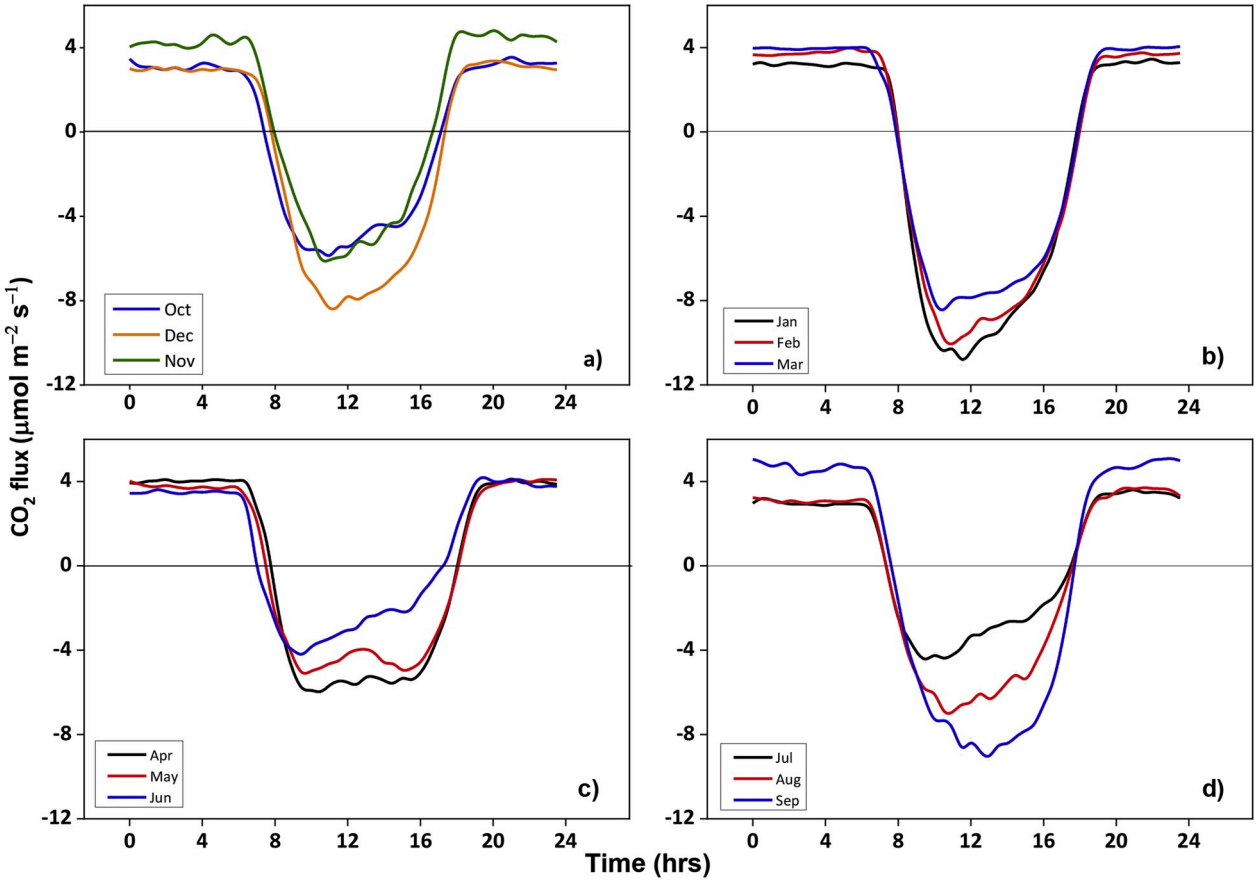

Fig. 6. Seasonal variation of diurnal patterns of CO_2 flux from October 2017 to September 2018. (a) Northeast monsoon season, (b) winter or post-monsoon season, (c) summer season, and (d) pre-monsoon season.

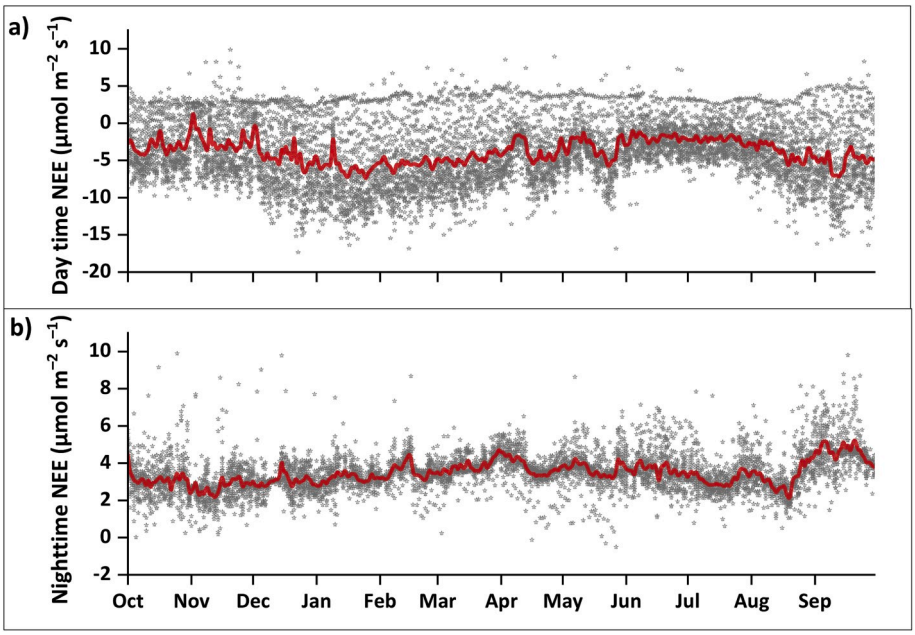

Fig. 7. Half-hourly (a) daytime and (b) night-time variations of NEE values on a monthly time scale. Red lines indicate the daily averages in each panel. (For interpretation of the references to color in this figure legend, the reader is referred to the Web version of this article.)

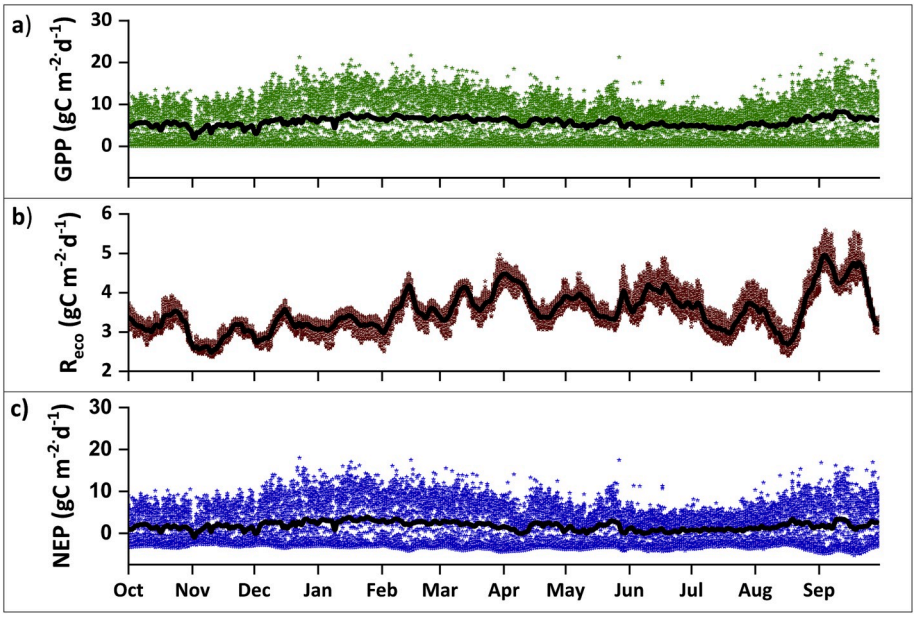

Fig. 8. The diurnal values of ecosystem fluxes on a monthly time scale were partitioned into (a) gross primary productivity (GPP), (b) ecosystem respiration (R_{eco}), and (c) net ecosystem production (NEP) during the whole study period. Black lines in panels (a–c) show the daily averages.

Table 1
Season-wise GPP, R_{eco}, and NEP values.

Season-wise periods	Rainfall (mm)	GPP(gC m^{-2} d^{-1})	R_{eco}(gC m^{-2} d^{-1})	NEP(gC m^{-2} d^{-1})
Northeast monsoon	468	3.46	3.06	0.39
Winter or post-monsoon (wet)	44	4.80	3.52	1.28
Summer (dry)	37	3.75	3.80	−0.05
Pre-monsoon	104	4.07	3.68	0.39

GPP: Gross primary productivity; R_{eco}: Ecosystem respiration; NEP: Net ecosystem productivity.

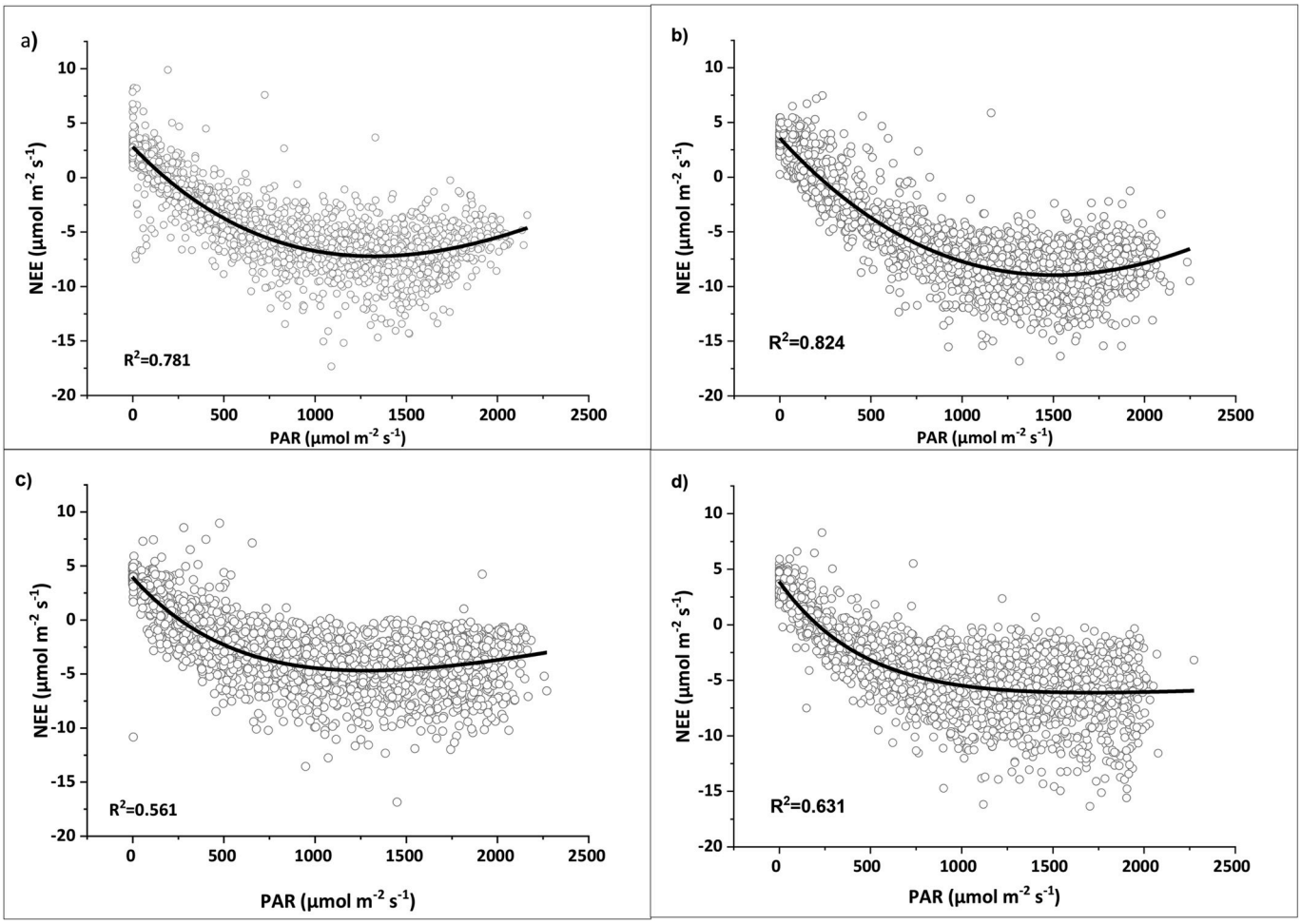

Fig. 9. Response between half-hourly daytime PAR and daytime NEE during different seasons: (a) October–December 2017, (b) January–March 2018; (c) April–June 2018; (d) July–September 2018.

time–averaged PAR values in the summer months ranged from 1451 to 1906 µmol m^{-2} s^{-1}, which affected the photosynthesis of the forest canopy (Fig. 9c). However, high NEE values were also observed during the pre-monsoon months of July–September due to the high rate of PAR (1333–1745 µmol m^{-2} s^{-1}), and this contributed to better carbon sequestration. Despite this, the ecosystem respiration increased from 2.7 to 5 µmol m^{-2} s^{-1}, and this caused an overall reduction in NEP during the pre-monsoon period (Fig. 9d).

Table 2
Average monthly variations in daytime NEE light response parameters from October 2017 to September 2018 in the Pichavaram mangrove ecosystem in south India.

Month	α (µmol CO_2 µmol photon^{-1})	Pmax (µmol CO_2 m^{-2} s^{-1})
Oct	−0.020	−13.35
Nov	−0.018	−13.23
Dec	−0.022	−19.67
Jan	−0.026	−21.33
Feb	−0.027	−19.24
Mar	−0.022	−18.8
Apr	−0.023	−14.13
May	−0.028	−12.16
Jun	−0.028	−8.91
Jul	−0.025	−9.01
Aug	−0.024	−14.73
Sep	−0.028	−21.55

α: Apparent quantum yield; NEE: net ecosystem exchange; Pmax: Maximum photosynthetic rate.

Regarding monthly variations in daytime NEE light response parameters (Table 2), the apparent quantum yield (α) and the maximum net photosynthetic rate (Pmax) showed similar trends. The maximum and minimum α values were observed in November and September, respectively. In general, α values in the summer season were higher than those during the northeast monsoon season (October–December). During the summer, the quantum yield of the ecosystem was high. But despite these characteristics, the relation between daytime NEE and PAR indicated that the Pmax increased during the winter or post-monsoon season but not during the summer season. Therefore, it is inferred that most of the annual carbon accumulated in our study site was during the wet season.

3.5. Relation between net ecosystem exchange and other environmental parameters

The daytime NEE responded to air temperature differently with season (Fig. 10a–d). For example, at a given temperature, the daytime NEE value was higher at a lower temperature (during January–March; 26.45 °C averaged) than at high temperatures (during the summer months of April–June; 30.57 °C averaged) (Fig. 10a–d). To examine the relations between the NEE and environmental parameters, we mapped monthly rainfall and water salinity (Fig. 11). The NEE and the VPD were also plotted to quantify the net carbon exchange patterns (Fig. 11). The NEP was also plotted as a function of air temperature, VPD, and salinity (Fig. 12a–c). It decreased linearly with both air temperature and VPD, but did not show a distinct pattern with salinity. NEP varied

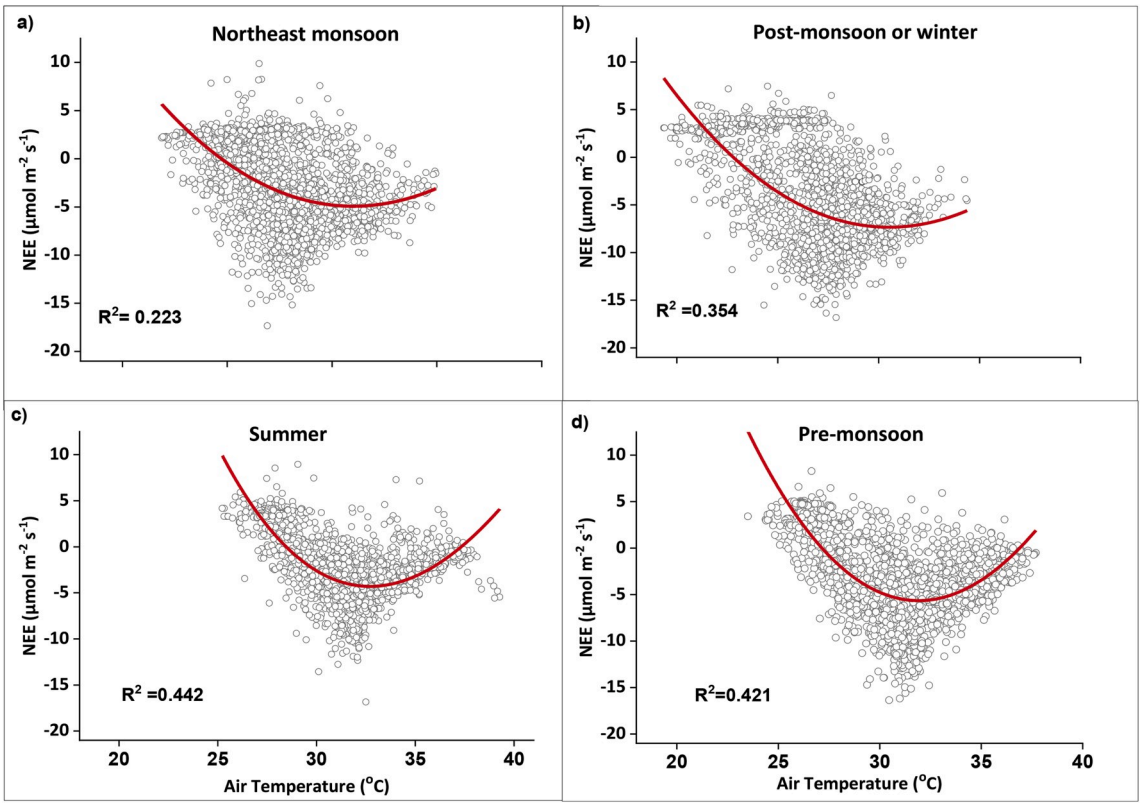

Fig. 10. Relation between half-hourly daytime air temperature and NEE in different seasons: (a) October–December 2017, (b) January–March 2018, (c) April–June 2018, and (d) July–September 2018.

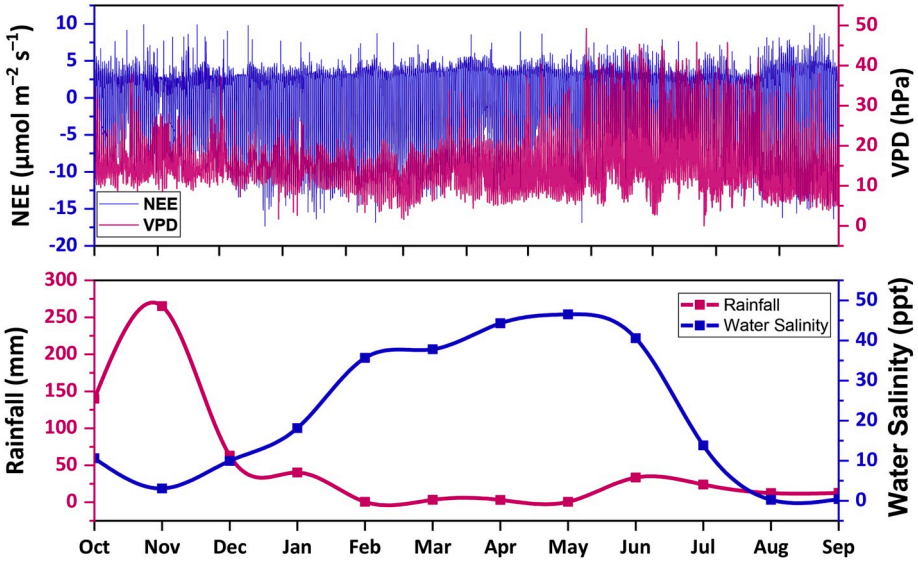

Fig. 11. The co-variation between the half-hourly NEE (blue) and VPD (purple) averaged on a monthly time scale during the study period (upper panel). The time profiles of the monthly mean of rainfall and water salinity have been shown in the lower panel. (For interpretation of the references to color in this figure legend, the reader is referred to the Web version of this article.)

considerably among the VPD regimes, with a significantly higher value over the medium VPD range of 10–20 hPa. According to the results, the carbon sink capacity decreased with increasing VPD; this was rapid when VPD was higher than 25 hPa. The fitted lines of NEP showed a significant difference between low and high salinity values (Fig. 12c). Further, the carbon sink capacity of our study area decreased with decreasing monthly rainfall and increased air temperature.

4. Discussion

4.1. Net ecosystem productivity estimates of south Indian tropical mangroves

Our results indicated that the maximum negative flux around or just before noon implied high photosynthetic activities under optimum solar net radiation associated with the CO_2 sequestration by the forest

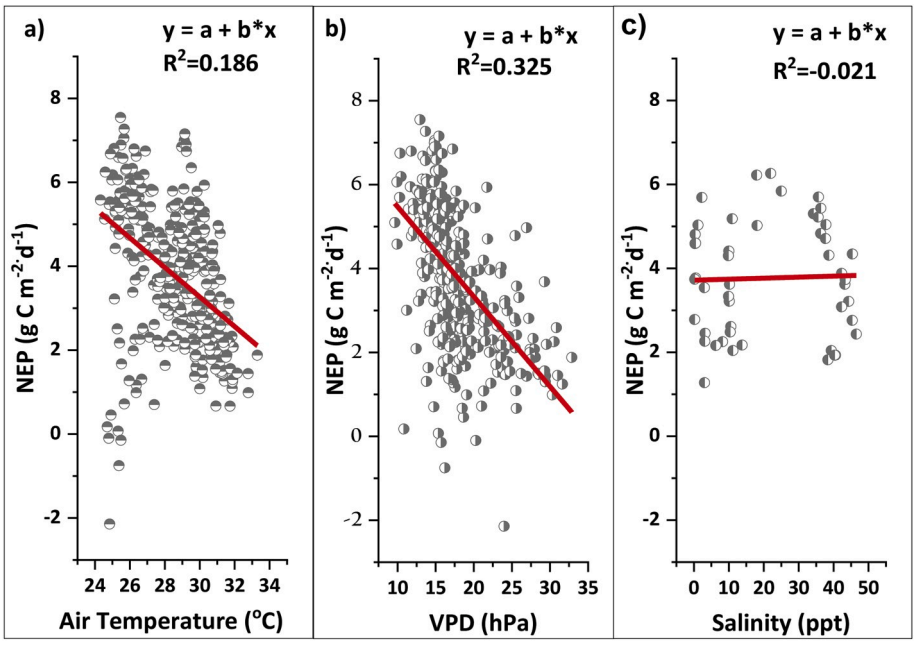

Fig. 12. Relationship between daytime NEP (gC m^{-2} d^{-1}) and (a) daytime averaged air temperature, (b) daytime averaged VPD, and (c) weekly averaged salinity. The NEP shows good inverse correlation with air temperature and VPD, but no systematic pattern is observed in the case of salinity. In the regression equation, the NEP is represented by y and the corresponding independent variable by x in each case.

canopies (Rodda et al., 2016; Chatterjee et al., 2018; Sarma et al., 2018). The positive night-time fluxes were lower in magnitude than the negative daytime fluxes, particularly during October–May, and August–September (Fig. 7a and b). However, the highest night-time positive fluxes (R_{eco}) were measured in the summer months, that is, during the months of June and July (Mildenberger et al., 2009). Rodda et al. (2016) reported that in the Sundarban mangrove forest, the peak negative CO_2 flux was −6.0 μmol m^{-2} s^{-1} observed during the daytime of summer 2012. Our estimation of −5 μmol m^{-2} s^{-1} (for daytime) is slightly lower than that observed by Rodda et al. (2016), as is the mean night-time positive flux (3.3 μmol m^{-2} s^{-1}). Our results are very similar to those seen in the "Coeur de Voh" mangroves in New Caledonia (−5 μmol m^{-2} s^{-1}; Leopold et al., 2016). However, our estimated annual NEP of the Pichavaram mangrove forest (183 gC m^{-2}) for October 2017–September 2018 is considerably higher than the reported values of "Coeur de Voh" dwarf mangroves, which are about 73.8 gC m^{-2} (Leopold et al., 2016). Based on the EC and biometric estimates in the Pichavaram mangroves, the current values are within the range indicated by Kathiresan et al. (2013). They estimated the carbon sequestration rate at the Pichavaram mangroves forest using the biometric-based method (BM) and reported that the values ranged between 1.1 and 8.0 t C ha^{-1} y^{-1} with different age groups of the mangroves across seasons. Rodda et al. (2016) reported a high NEP of about 249 gC m^{-2} y^{-1} at the Sundarban mangroves. This could be attributed to the low respiration rate of 2–4 μmol m^{-2} s^{-1} and, to some extent, to the tidal activity in this region, which sometimes rises as high as 1 m. Additionally, consistent freshwater discharges (from the river) make the water level high around the tower site, which turns the soil anoxic and may have contributed to the low respiration rate in Sundarbans. However, in the Pichavaram mangroves, we measured a higher respiration rate varying from 2.42 to 4.96 μmol m^{-2} s^{-1} with high soil temperatures (25°C–35 °C) (Fig. 8b). During the rainy season, the Pichavaram forest soil gets inundated by river flood discharges, which suppress the soil respiration. During the rest of the season, the soil remains somewhat dry, leading to higher soil respiration (Gnanamoorthy et al., 2019). Cui et al. (2018) also compared the two different ecosystems of mangrove wetlands and terrestrial forests from the subtropical region of China. Their results showed that the mangrove wetlands sequester more carbon than the terrestrial forests because of higher gross ecosystem production (GEP) and lower decomposition rates in soil organic carbon, resulting in lower soil respiration in mangroves than in the terrestrial forests.

On the other hand, the estimated NEP of the Florida Everglades mangrove forests is very high at about 1170 ± 145 gC m^{-2} y^{-1}, but these mangroves have a high density of trees with heights greater than 25 m and higher above- and below-ground biomasses with different species composition varying from *Rhizophora mangle, Avicennia germinans*, and *Laguncularia racemosa* (Simard et al., 2006; Barr et al., 2010). Liu and Lai (2019) also quantified the annual carbon uptake rates of a mangrove forest dominated by *Kandelia obovata* in the subtropical region of China. The values ranged from 758 to 890 gC m^{-2} y^{-1}, which were higher than those in the tropical ecosystem of the Pichavaram mangroves. The high values could be attributed to their higher mean canopy height of approximately 6.5 m, with a mean diameter at breast height (DBH) of 7.6 cm, and a tree density of 0.7 individuals per square meter. In contrast, the Pichavaram mangrove has a smaller canopy with an average height of approximately 3 m (LAI ranged from 0.8 to 2 m^2 m^{-2}) with a single dominant species of *A. marina* (74%) (Selvam et al., 2002).

4.2. CO_2 flux response to environmental controls

4.2.1. Influence of air temperature

A recent global analysis highlighted that precipitation, temperature, salinity, and tidal pattern are the major influencing factors at local and regional levels for mangrove growth (Alongi, 2002; Barr et al., 2010; Saintilan et al., 2014; Leopold et al., 2016; Simard et al., 2019). In our study, the air temperature during the summer months had greatly affected the NEE pattern than the temperature during the wet months, which had a positive influence on ecosystem respiration and negative influence on NEP (Fig. 10a–d). In our mangrove site, the daytime air temperature remains high (>35 °C) during the summer season. Nandy and Ghose (2005) demonstrated that *A. marina* had photosynthetic capacity till 36.6 °C of canopy temperature; our results also showed clear evidence of carbon sources under a higher air temperature (>35 °C). Gilman et al. (2008) reported an optimum air temperature range (28°C–32 °C) for carbon uptake of mangroves species, but our observation showed higher values than those observed during the summer

months, which ultimately decreased the carbon fixation capacity of the mangroves. Futher, Niu et al. (2012) reported that high temperatures could reduce GPP through a reduction in stomatal conductance in response to the higher evaporative demands and lower soil water contents. A recent study by Liu and Lai (2019) conducted in a Chinese subtropical mangrove wetland showed that the temperature had dominant control of the temporal variations in CO_2 flux in the wet seasons than in the dry seasons, which resulted in an overall increase in ecosystem respiration and decrease in net carbon uptake during the wet period.

4.2.2. *Influence of photosynthetically active radiation on net ecosystem exchange in mangrove ecosystems*

Net ecosystem exchange response to the proportion of PAR depends on seasonal patterns (Fig. 9a–d). During the daytime, the NEE light response parameter α in the summer months (April–June) was higher than that during the northeast monsoon season (October–December). Despite this, more carbon assimilation occurred during the wet months than during the summer period in our study area. A similar pattern was also noted by Barr et al. (2010) in the Everglades mangroves in Florida. Their finding shows that the positive effects of diffuse solar irradiance at minimum NEE values occurred when PAR varied between 1400 and 2100 μmol $m^{-2}s$-^{1} with slightly elevated air temperature ranging from 24 °C to 28 °C. Furthermore, Barr et al. (2010) pointed out that leaf orientation was another factor influencing the PAR on NEE during the summer months; sunlight can tilt mangrove foliage in a more vertical direction (up to 75° from the horizontal) compared to shaded foliage. The foliage angle of sun-exposed mangrove leaves varies among species (Lovelock and Clough, 1992). A tilted leaf can reduce direct solar radiation, allowing them to remain at temperatures that are favorable for photosynthesis (Ball, 1988; Farnsworth and Ellison, 1996). Yu et al. (2008) also stated that the climatic conditions and GEP values of the terrestrial forests were mainly controlled through PAR and air temperature. The "Coeur de Voh" mangroves of New Caledonia are characterized by a semi-arid climate. Here, the response of daytime NEE to PAR differed depending on the air temperature. The NEE values decreased and then increased with increasing air temperature (Leopold et al., 2016); similar patterns were also observed in other mangroves (Barr et al., 2013b; Chen et al., 2014). Similar to our results, Rodda et al. (2016) also recorded a higher quantum yield during the monsoon month (September), which provided favorable conditions for the growth of the Indian Sundarban mangroves. Lower quantum yields were observed in the hotter month of May, resulting in a reduction of the NEE due to higher PAR. The light use efficiency (LUE) in the Mai Po Nature Reserve (Hong Kong, China) mangrove canopy decreased with an increase in both air temperature and VPD. At Pichavaram, our results showed that a higher light response parameter limited the NEE values of the mangroves (Table 2).

4.2.3. *Control of rainfall*

In our study site, the NEE values were found to be highly varying with seasonal patterns, due to various environmental factors such as higher net radiation, low rain events, hypersaline water, and freshwater inflow into the mangrove forest from the river. The Pichavaram mangrove forest typically receives an average annual rainfall of about 1310 mm (Selvam, 2003), but during the study period, the total rainfall received was half of this value. The estimated annual evapotranspiration (ET) during the study period was 610 mm, whereas the precipitation was 653 mm (much dryer than the long-term average) (Fig. S2). A compilation of the global data set from tropical and subtropical mangrove forests shows that the annual NEP of mangroves maintains an increasing trend with yearly precipitation (Fig. 13). Furthermore, the Everglades mangroves in Florida were found to have a similar pattern. Barr et al. (2010) observed that the higher rainfall caused a decrease in soil effluxes but increased the NEP due to the combined effects of increased freshwater discharge and long-term low saline water inundation. Meanwhile, Leopold et al. (2016) found that a higher rainfall pattern helped increase both GPP and R_{eco} but reduced NEP during the wet seasons when compared with the dry periods in the "Coeur de Voh" mangrove, New Caledonia. Similarly, Liu and Lai (2019) estimated that the GPP level in a humid Hong Kong mangrove was reduced by 32.6% due to heavy precipitation. They attributed this to the reduction in the photosynthetic photon flux density (PPFD) compared with the non-rainy days. The NEE during the non-rainy days in this region was found to be enhanced by more than 100% (Liu and Lai, 2019). Similarly, our study site also recorded lower NEP during the monsoon season (October–December) than in the post-monsoon period (January–March), presumably driven by the lower PAR during the former period. During these months, both the GPP (3.18 gC m^{-2} d^{-1}) and R_{eco} (3.06 gC m^{-2} d^{-1}) were observed in high values were ultimately reduced the NEP (Fig. 8a–c). The influence of rainfall patterns was compared with the October–December, and January–March data sets. The NEP and PAR values during these two seasons varied greatly from 0.39 to 3.22 gC m^{-2} d^{-1} and 680–938 μmol m^{-2} s^{-1}, respectively.

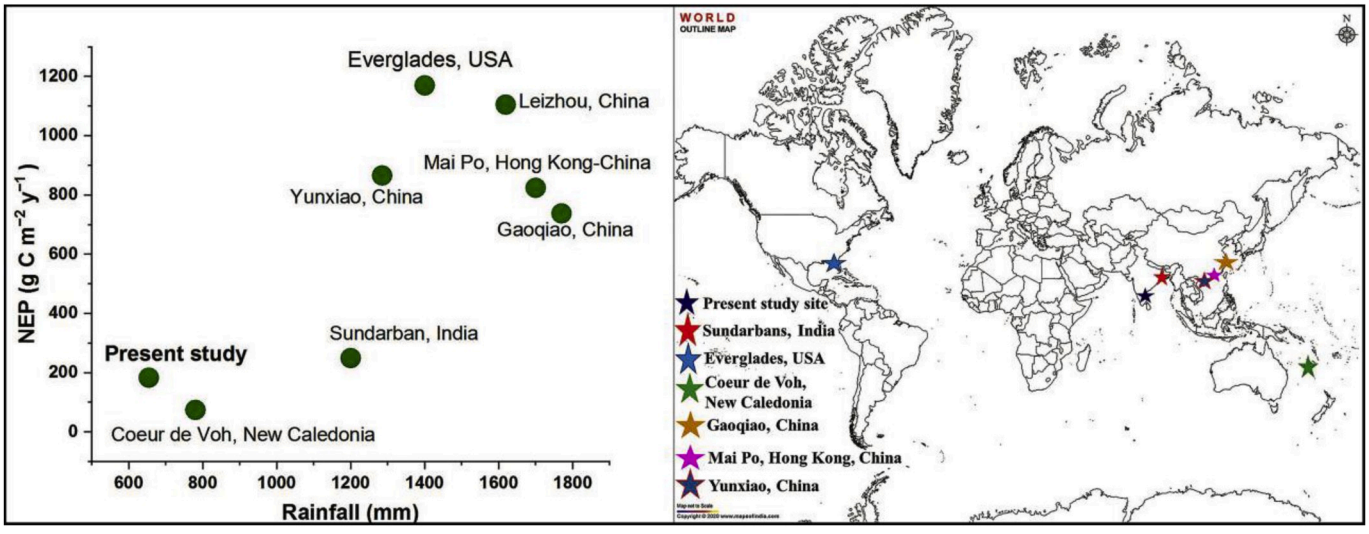

Fig. 13. The eddy covariance based estimates of annual net ecosystem production (NEP, gC m^{-2}) and annual precipitation (mm) in different mangrove wetlands sites from tropical and subtropical regions of world. Data from Barr et al. (2010), Chen et al. (2014), Rodda et al. (2016), Leopold et al. (2016), Cui et al. (2018), and Liu and Lai (2019).

4.2.4. Influence of vapor pressure deficit and water salinity

Vapor pressure deficit is possibly one of the important environmental factors for transpiration and mangrove plant growth and development (Oren et al., 1999; Leuschner, 2002). A number of studies have indicated that mangroves are highly responsive to changes in lower and higher VPD leading to stomatal closure, which can lower the cost of carbon gain in the mangroves (Cheeseman and Lovelock, 2004; Barr, 2005; Naidoo, 2006; Alongi, 2009; Keith et al., 2012). Chen et al. (2014) stated that VPD and air temperature were important secondary factors controlling the daytime NEE values, especially after a typhoon. They found that low GPP values due to typhoons were likely to reduce the carbon assimilation under high VPD and air temperature conditions. Goulden et al. (2004) also demonstrated that the positive influence between NEE fluxes and VPD was caused by elevated air temperature and higher VPD. In our study, we found that lower NEE values were observed when VPD exceeded 25 hPa, and the temperature was higher than 35 °C, suggesting that stomatal closure and a decrease in carbon fixation occurred when these values were high (Figs. 11 and 12a–b). The tropical and subtropical mangrove carbon assimilation rates were likely to decrease when the air temperature and VPD were at their maximum, as shown in studies by Barr et al. (2010, 2013b), Leopold et al. (2016), and Liu and Lai (2019).

The carbon balance in mangrove forests is thus partially influenced by the physical conditions that regulate salinity in coastal environments (Barr et al., 2010). Salinity is an important factor regulating photosynthesis and stomatal conductance in mangroves, as reported by several investigators (Takemura et al., 2000; Parida et al., 2004; Lopez-Hoffman et al., 2006). Similar to the New Caledonia mangroves (Leopold et al., 2016), the Pichavaram mangrove wetlands are also characterized by two distinct spatially distributed zones of flora. The *Avicennia* zone developed behind the *Rhizophora* zone with higher elevations in the intertidal area. The tidal amplitude range around our EC flux tower is very limited (between 50 and 25 cm) and depends on the season (Selvam et al., 2002); therefore, tidal inundation in the *Avicennia* zone occurs only during the northeast monsoon season (October–December) and thereafter freshwater is discharged from the river (mostly during July–September). In our study site, creek water salinity showed high seasonal variation: it was much lower during the northeast monsoon and pre-monsoon (July–September) seasons than in the summer months (Fig. 11). During the northeast monsoon season, the decrease in salinity was clearly related to rainfall and freshwater input. In this connection, our study observed the hypersalinity conditions during March–May due to reduced tidal water or no freshwater input from rainfall. Consequently, the creek water experiences hypersalinity during the summer months ranging between 38 and 47 ppt (Fig. 11). Under a low rainfall regime, the salinity increased, and as a result, the carbon sequestration capacity was reduced. *Avicennia*, one of a wide range of salt-tolerant mangrove species, used the saline water to overcome drying and reduce saline stress conditions (Martin et al., 2010; Morrisey et al., 2010). Under higher salinity, mangrove plants have the adaptation mechanisms to lower the stem hydraulic conductivity that restricts the flow rates but also reduce vulnerability of xylem vessels to cavitation (Sperry et al., 1988; Melcher et al., 2001). Thus, the supply of water to leaves through roots and stems could be lowered under hypersaline conditions, which consequently reduces the photosynthetic rate. In our study also shows that reduction stomatal conductance and reduced photosynthetic activities made the ecosystem a carbon source during the summer. There was a negative relationship between NEP and water salinity across all seasons in our study (Fig. 12c). Leopold et al. (2016) also observed that the decreased GPP level during the dry season when compared with the wet season, due to less water availability in terms of no rainfall and least tidal inundation, correlated with higher pore water salinity in the dwarf mangroves of New Caledonia. Cui et al. (2018) reported that the hypersaline conditions of the mangroves had greatly influenced the LUE, but the relationship between salinity and LUE was different based on the site and salinity range. In our site, which experienced low salinity conditions during July–September, salinity (0.4–14 ppt) was reduced even without rainfall. This was mainly attributed to the mangrove forest floor being fully inundated with freshwater discharge from the river Coleroon of the Cauvery delta (https://sandrp.in/2018/07/24/cauvery-is-facing-very-serious-flood-risk-but-cwc-is-in slumber/). Liu and Lai (2019) found that water salinity (1–17 ppt) had a positive effect on both LUE and GPP in the subtropical mangroves of Hong Kong, China. Similarly, in our study, we observed that the lower salinity showed an increase in GPP, particularly in October–January (3–25 ppt) and July–September (0.23–13.8 ppt). Additionally, salinity can influence soil carbon decomposition through soil respiration (Robertson and Alongi, 2016; Gnanamoorthy et al., 2019). In this study, R_{eco} under high salinity was significantly higher than that under low salinity, as seen from the higher R_{eco} (3.8 gC m^{-2} d^{-1}) observed in higher saline environments due to non-flooding conditions during the summer periods. The negative effect of salinity on R_{eco} has been seen in some other wetlands as demonstrated by studies stating that R_{eco} was found to be significantly lower under high salinity conditions than under low salinity conditions (Liu and Lai, 2019). Increased R_{eco} under low salinity conditions (4.36 gC m^{-2} d^{-1}) was observed in our study as well. This was only in September after the freshwater input from the river, which could have diluted the saline water and subsequently lowered water salinity to give optimum conditions for higher soil respiration (Fig. 8b). Overall, we found that the Pichavaram mangrove ecosystem acted as a carbon sink of 1.83 tC ha^{-1} y^{-1}during the observation period. Approximately 95% of carbon was sequestered during the winter or post-monsoon and pre-monsoon seasons. It was nearly carbon neutral during the northeast monsoon season and acted as a net source during the summer months. Therefore, it is very important to consider the impact of future climate changes on the carbon exchange of such a mangrove ecosystem, as it may be highly sensitive to changes in rainfall, salinity, and temperature.

5. Conclusions

The EC technique was used to determine carbon exchange over the Pichavaram mangrove ecosystem on the southeast coast of India from October 2017 to September 2018. The results show that the Pichavaram mangrove forest, on an annual time scale, acted as a moderate sink of atmospheric carbon, with an annual average NEP of 183 gC m^{-2}. This value is similar to that of other Indian mangrove forests, such as the Sundarbans, but considerably lower than those reported from other mangrove ecosystems across the world. One reason for this low value is vegetation characteristics. The mangrove trees in Pichavaram are considerably shorter in height when compared with those in other locations. However, other factors, such as the elevated air temperature, rainfall pattern, and hypersalinity of the area during the summer season, also played a significant role. Further investigations are required to better characterize the role of rainfall in carbon sequestration processes in this ecosystem. Nevertheless, the present estimates of NEP, GPP, and R_{eco} are within the range of values reported from terrestrial ecosystems across the world. However, the carbon sink capability may decline in the future based on rising temperatures, decreasing rainfall, variable salinity, and tidal inundation patterns. Consequently, long-term studies are required to evaluate how environmental parameters, including the estuarine tidal exchange of aquatic carbon species driven by climate change, would influence the carbon and water fluxes in this fragile ecosystem.

Declaration of competing interest

The authors declare that they have no known competing financial interests or personal relationships that could have appeared to influence the work reported in this paper.

CRediT authorship contribution statement

Palingamoorthy Gnanamoorthy: Conceptualization, Data curation, Formal analysis, Writing - original draft. **V. Selvam:** Conceptualization, Funding acquisition. **Pramit Kumar Deb Burman:** Data curation, Formal analysis, Writing - original draft. **S. Chakraborty:** Conceptualization, Data curation, Formal analysis, Writing - original draft. **A. Karipot:** Conceptualization. **R. Nagarajan:** Writing - review & editing. **R. Ramasubramanian:** Writing - original draft. **Qinghai Song:** Writing - review & editing. **Yiping Zhang:** Writing - review & editing. **John Grace:** Data curation, Formal analysis, Writing - original draft.

Acknowledgments

This work is part of the MetFlux India Project initiated by the Indian Institute of Tropical Meteorology, Pune. The Ministry of Earth Sciences, Government of India, is acknowledged for financial support. We also thank the Tamil Nadu Forest Department for providing the necessary permission. We are grateful to the founder Chairman and Chairperson of MSSRF for providing the facilities necessary for this work.

Appendix A. Supplementary data

Supplementary data to this article can be found online at https://doi.org/10.1016/j.ecss.2020.106828.

References

Alongi, D.M., 2002. Present state and future of the world's mangrove forests. Environ. Conserv. 29, 331–349.
Alongi, D.M., 2009. The Energetics of Mangrove Forests. Springer, Dordrecht. https://doi.org/10.1007/978-1-4020-4271-3.
Alongi, D.M., 2014. Carbon cycling and storage in mangrove forests. Ann. Rev. Mar. Sci. 6, 195–219.
Aubinet, M., Chermanne, B., Vandenhaute, M., Longdoz, B., Yernaux, M., Laitat, E., 2001. Long term carbon dioxide exchange above a mixed forest in the Belgian Ardennes. Agric. For. Meteorol. 108, 293–315.
Balachandran, S., Asokan, R., Sridharan, S., 2006. Global surface temperature in relation to northeast monsoon rainfall over Tamil Nadu. J. Earth Syst. Sci. 115, 349–362.
Baldocchi, D.D., 1997. Measuring and modelling carbon dioxide and water vapour exchange over a temperate broad-leaved forest during the 1995 summer drought. Plant Cell Environ. 20, 1108–1122.
Baldocchi, D., 2003. Assessing the eddy covariance technique for evaluating carbon dioxide exchange rates of ecosystems: past, present and future. Global Change Biol. 9, 479–492.
Baldocchi, D., Finnigan, J., Wilson, K., Paw, U.K.T., Falge, E., 2000. On measuring net ecosystem carbon exchange over tall vegetation on complex terrain. Bound. Lay. Meteorol. 96, 257–291.
Ball, M.C., 1988. Ecophysiology of mangroves. Trees 2, 129–142.
Barr, J.G., 2005. Carbon Sequestration by Riverine Mangroves in the Florida Everglades, PhD Thesis. University of Virginia, Charlottesville, p. 183.
Barr, J.G., Engel, V., Fuentes, J.D., Zieman, J.C., O'Halloran, T.L., Smith, T.J., Anderson, G.H., 2010. Controls on mangrove forest-atmosphere carbon dioxide exchanges in western Everglades National Park. J. Geophys. Res. 115, G02020.
Barr, J.G., Engel, V., Smith III, T.J., Fuentes, J.D., 2012. Hurricane disturbance and recovery of energy balance, CO_2 fluxes and canopy structure in a mangrove forest of the Florida Everglades. Agric. For. Meteorol. 153, 54–66.
Barr, J.G., Fuentes, J.D., DeLonge, M.S., O'Halloran, T.L., Barr, D., Zieman, J.C., 2013a. Summertime influences of tidal energy advection on the surface energy balance in a mangrove forest. Biogeosciences 10, 501–511.
Barr, J.G., Engel, V., Fuentes, J.D., Fuller, D.O., Kwon, H., 2013b. Modeling light use efficiency in a subtropical mangrove forest equipped with CO_2 eddy covariance. Biogeosciences 10, 2145–2158.
Barr, J.G., DeLonge, M.S., Fuentes, J.D., 2014. Seasonal evapotranspiration patterns in mangrove forests. J. Geophys. Res. Atmos. 119, 3886–3899.
Beer, C., Reichstein, M., Tomelleri, E., Ciais, P., Jung, M., Carvalhais, N., Rödenbeck, C., Altaf Arain, M., Baldocchi, D., Bonan, G.B., Bondeau, A., Cescatti, A., Lasslop, G., Lindroth, A., Lomas, M., Luyssaert, S., Margolis, H., Oleson, K.W., Roupsard, O.E., Veenendaal, E., Viovy, N., Williams, C., Woodward, F.I., Papale, D., 2010. Terrestrial gross carbon dioxide uptake: global distribution and covariation with climate. Science 329, 834–838.
Bonan, G.B., 2008. Forests and climate change: forcings, feedbacks, and the climate benefits of forests. Science 320 (5882), 1444–1449.
Bouillon, S., Borges, A.V., Moya, E.C., Diele, K., Dittmar, T., Duke, N.C., Kristensen, E., Lee, S.Y., Marchand, C., Middelburg, J.J., Rivera-Monroy, V.H., Smith III, T.J., Twilley, R.R., 2008. Mangrove production and carbon sinks: a revision of global budget estimates. Global Biogeochem. Cycles 22, GB2013.
Burba, G., 2013. Eddy Covariance Method for Scientific, Industrial, Agricultural, and Regulatory Applications: a Field Book on Measuring Ecosystem Gas Exchange and Arial Emission Rates. LI-COR Biosciences, Lincoln, NE, USA, p. 331.
Chanda, A., Akhand, A., Manna, S., Dutta, S., Hazra, S., Das, I., Dadhwal, V.K., 2013. Characterizing spatial and seasonal variability of carbon dioxide and water vapour fluxes above a tropical mixed mangrove forest canopy. India J. Earth Syst. Sci. 122, 503–513.
Chatterjee, A., Roy, C., Chakraborty, A., Sarkar, S., Singh, C., Karipot, S., Ghosh, A.K., Mitra, A., Raha, S., 2018. Biosphere atmosphere exchange of CO_2, H_2O vapour and energy during spring over a high altitude Himalayan forest at eastern India. Aerosol. Air Qual. Res. 18, 2704–2719.
Cheeseman, J.M., Lovelock, C.E., 2004. Photosynthetic characteristics of dwarf and fringe *Rhizophora mangle* L: in a Belizean mangrove. Plant Cell Environ. 27, 769–780.
Chen, H., Lu, W., Yan, G., Yang, Z., Lin, G., 2014. Typhoons exert significant but differentials impacts on net ecosystem carbon exchange of subtropical mangrove forests in China. Biogeosciences 11, 5323–5333.
Cui, X., Liang, J., Lu, W., Chen, H., Liu, F., Lin, G., Xu, F., Luo, Y., Lin, G., 2018. Stronger ecosystem carbon sequestration potential of mangrove wetlands with respect to terrestrial forests in subtropical China. Agric. For. Meteorol. 249, 71–80.
Dai, Z., Trettin, C.C., Frolking, S., Birdsey, R.A., 2018. Mangrove carbon assessment tool: model development and sensitivity analysis. Estuar. Coast Shelf Sci. 208, 23–35.
Deb Burman, P.K., Sarma, D., Williams, M., Karipot, A., Chakraborty, S., 2017. Estimating gross primary productivity of a tropical forest ecosystem over north-east India using LAI and meteorological variables. J. Earth Syst. Sci. 126 (7), 1–13.
Deb Burman, P.K., Sarma, D., Morrison, R., Karipot, A., Chakraborty, S., 2019. Seasonal variation of evapotranspiration and its effect on the surface energy budget closure at a tropical forest over north-east India. J. Earth Syst. Sci. 128 (5), 1–21.
Deb Burman, P.K., Shurpali, N.J., Prabha, T.V., Karipot, A., Chakraborty, S., Linda, S.E., Martikainen, P.J., Chellappan, S., Arola, A., Tiwari, Y.K., Murugavel, P., Gurnule, D., Todekar, K., Prabha, T.V., 2020a. CO_2 exchange from two different agro-ecosystems located in subtropical (India) and boreal (Finland) climatic conditions. J. Earth Syst. Sci. 129 (1), 43.
Deb Burman, P.K., Sarma, D., Chakraborty, S., Karipot, A., Jain, A.K., 2020b. The effect of Indian summer monsoon on the seasonal variation of carbon sequestration by a forest ecosystem over north-east India. SN Appl. Sci. 2 (2), 154.
Falge, E., Baldocchi, D., Olson, R., Anthoni, P., Aubinet, M., Bernhofer, C., Burba, G., Ceulemans, R., Clement, R., Dolman, H., Granier, A., Gross, P., Grünwald, T., Hollinger, D., Jensen, O., Katul, G., Keronen, P., Kowalski, A., TaLai, C., Law, B., Meyers, T., Moncrieff, J., Moors, E., Munger, W., PilegaardK, ., Rannik, U., Rebmann, C., Suyker, A., Tenhunen, J., Tu, K., Verma, S., Vesala, T., Wilson, K., Wofsy, S., 2001. Gap filling strategies for defensible annual sums of net ecosystem exchange. Agric. For. Meteorol. 107, 43–69.
Farnsworth, E.J., Ellison, A.M., 1996. Sun-shade adaptability of the red mangrove, *Rhizophora mangle* (Rhizophoraceae): changes through ontogeny at several levels of biological organization. Am. J. Bot. 83, 1131–1143.
Fei, X., Song, Q., Zhang, Y., Liu, Y., Sha, L., Yu, G., Zhang, L., Duan, C., Deng, Y., Wu, C., Lu, Z., Luo, K., Chen, A., Xu, K., Liu, W., Huang, H., Jin, Y., Zhou, Li, J., Lin, Y., Zhou, L., Fu, Y., Bai, X., Tang, X., Gao, J., Zhou, W., Grace, J., 2018. Carbon exchanges and their responses to temperature and precipitation in forest ecosystems in Yunnan, Southwest China. Sci. Total Environ. 616–617, 824–840.
Ganguly, D., Dey, M., Mandal, S.K., Dey, T.K., Jana, T.K., 2008. Energy dynamics and its implication to biosphere: atmosphere exchange of CO_2, H_2O and CH_4 in a tropical mangrove forest canopy. Atmos. Environ. 42, 4172–4184.
Gilman, E.L., Ellison, J., Duke, N.C., Field, C., 2008. Threats to mangroves from climate change and adaptation options: a review. Aquat. Bot. 89, 237–250.
Gnanamoorthy, P., Selvam, V., Ramasubramanian, R., Nagarajan, R., Chakraborty, S., Deb Burman, P., Karipot, A., 2019. Diurnal and seasonal patterns of soil CO_2 efflux from the Pichavaram mangroves, India. Environ. Monit. Assess. 191, 258.
Gnanappazhama, L., Selvam, V., 2014. Response of mangroves to the change in tidal and fresh water flow: a case study in Pichavaram, South India. Ocean Coast Manag. 102, 131–138.
Goulden, M.L., Munger, J.W., Fan, S.M., Daube, B.C., Wofsy, S.C., 1996. Measurements of carbon sequestration by long-term eddy covariance: methods and a critical evaluation of accuracy. Global Change Biol. 2, 169–182.
Goulden, M.L., Miller, S.D., Da Rocha, H.R., Menton, M.C., De Freitas, H.C.E., Silva Figueira, A.M., Dias De Sousa, C.A., 2004. Diel and seasonal patterns of tropical forest CO_2 exchange. Ecol. Appl. 14 (4 Suppl. L), 42–54.
Grace, J., Lloyd, J., McIntyre, J., Miranda, A.C., 1995. Carbon dioxide uptake by an undisturbed tropical rain forest in southwest Amazonia, 1992 to 1993. Science 270, 778–780.
Hanson, P.J., Amthor, J.S., Wullschleger, S.D., Wilson, K.B., Grant, R.F., Hartley, A., Hui, D., Hunt, E.R., Johnson, D.W., Kimball, J.S., King, A.W., Luo, Y., Mcnulty, S.G., Sun, G., Thornton, P.E., Wang, S., Williams, M., Baldocchi, D.D., Cushman, R.M., 2004. Carbon and water cycle simulations for an upland oak forest using 13 stand-level models: intermodel comparisons and evaluations against independent measurements. Ecol. Monogr. 74, 443–489.
IMD (India Met Dept, 1973. Northeast monsoon. FMU Rep. No. IV 18, 4.
IPCC, 2013. In: Stocker, T.F., Qin, D., Plattner, G.-K., Tignor, M., Allen, S.K., Boschung, J., Nauels, A., Xia, Y., Bex, V., Midgley, P.M. (Eds.), Climate Change 2013: the Physical Science Basis. Contribution of Working Group I to the Fifth Assessment Report of the Intergovernmental Panel on Climate Change. Cambridge University Press, Cambridge, United Kingdom and New York, United States.
Jennerjahn, T.C., Gilman, E., Krauss, K.W., Lacerda, L.D., Nordhaus, I., Wolanski, E., 2017. Mangrove ecosystems under climate change. In: Rivera-Monroy, V.H., Lee, S. Y., Kristensen, E., Twilley, R.R. (Eds.), Mangrove Ecosystems: a Global Biogeographic Perspective. Springer, Cham Online, ISBN 978-3-319-62206-4.

Jha, C.S., Thumaty, K.C., Rodda, S.R., Sonakia, A., Dadhwal, V.K., 2013. Analysis of carbon dioxide, water vapour and energy fluxes over an Indian teak mixed deciduous forest for winter and summer months using eddy covariance technique. J. Earth Syst. Sci. 122, 1259–1268.
Jha, C.S., Rodda, S.R., Thumaty, K.C., Raha, A.K., Dadhwal, V.K., 2014. Eddy covariance based methane flux in Sundarbans mangroves. India J. Earth Syst. Sci. 123, 1089–1096.
Kathiresan, K., 2000. A review of studies on Pichavaram mangrove, Southeast India. Hydrobiologia 430, 185–205.
Kathiresan, K., Anburaj, R., Gomathi, V., Saravanakumar, K., 2013. Carbon sequestration potential of *Rhizophora mucronata* and *Avicennia marina* as influenced by age, season, growth and sediment characteristics in southeast coast of India. J. Coast Conserv. 17, 397–408.
Keith, H., van Gorsel, E., Jacobsen, K., Cleugh, H., 2012. Dynamics of carbon exchange in a eucalyptus forest in response to interacting disturbance factors. Agric. For. Meteorol. 153, 67–81.
Kolari, P., Pumpanen, J., Rannik, U., Ilvesniemi, H., Hari, P., Berninger, F., 2004. Carbon balance of different aged Scots pine forests in southern Finland. Global Change Biol. 10, 1106–1119.
Law, B.E., Waring, R.H., Anthoni, P.M., Aber, J.D., 2000. Measurement of gross and net ecosystem productivity and water vapor exchange of a *Pinus ponderosa* ecosystem, and an evaluation of two generalized models. Global Change Biol. 6, 155–168.
Lei, H.M., Yang, D.W., 2010. Seasonal and interannual variations in carbon dioxide exchange over a cropland in the North China Plain. Global Change Biol. 16, 2944–2957.
Leopold, A., Marchand, C., Renchon, A., Deborde, J., Quiniou, T., Allenbach, M., 2016. Net ecosystem CO_2 exchange in the "Coeur de Voh" mangrove, New Caledonia: effects of water stress on mangrove productivity in a semi-arid climate. Agric. For. Meteorol. 223, 217–232.
Leuschner, C., 2002. Air humidity as an ecological factor for woodland herbs: leaf water status, nutrient uptake, leaf anatomy, and productivity of eight species grown at low or high VPD levels. Flora 197, 264–274.
Li, Q., Lu, W., Chen, H., Luo, Y., Lin, G., 2014. Differential responses of net ecosystem exchange of carbon dioxide to light and temperature between spring and neap tides in subtropical mangrove forests. Scientif. World J., 943697
Liu, J., Lai, D.Y.F., 2019. Subtropical mangrove wetland is a stronger carbon dioxide sink in the dry than wet seasons. Agric. For. Meteorol. 278, 107644.
Lovelock, C.E., Clough, B.F., 1992. Influence of solar radiation and leaf angle on leaf xanthophyll concentrations in mangroves. Oecologia 91, 518–525.
Lopez Hoffman, L., DeNoyer, J.L., Monroe, I.E., Shaftel, R., Anten, N.P.R., Martinez-Ramos, M., Ackerly, D.D., 2006. Mangrove seedling net photosynthesis, growth, and survivorship are interactively affected by salinity and light. Biotropica 38 (5), 606–616.
Martin, K.C., Bruhn, D., Lovelock, C.E., Feller, I.C., Evans, J.R., Ball, M.C., 2010. Nitrogen fertilization enhances water-use efficiency in a saline environment. Plant Cell. Environ 33, 344–357.
Melcher, P.J., Goldstein, G., Meinzer, F.C., Yount, D.E., Jones, T.J., Holbrook, N.M., Huang, C.X., 2001. Water relations of coastal and estuarine *Rhizophora mangle*: xylem pressure potential and dynamics of embolism formation and repair. Oecologia 126, 182–192.
Mildenberger, K., Beiderwieden, E., Hsia, Y.J., Klemm, O., 2009. CO_2 and water vapor fluxes above a subtropical mountain cloud forest: the effect of light conditions and fog. Agric. For. Meteorol. 149, 1730–1736.
Morrisey, D., Swales, A., Dittmann, S., Morrison, M., Lovelock, C.E., Beard, C., 2010. The ecology and management of temperate mangroves. Oceanogr. Mar. Biol. Annu. Rev. 48, 43–160.
Mukhopadhyay, S.K., Jana, T.K., De, T.K., Sen, S., 2000. Measurement of exchange of CO_2 in mangrove forest of Sundarbans using micrometeorological method. Trop. Ecol. 41, 57–60.
Naidoo, G., 2006. Factors contributing to dwarfing in the mangrove *Avicennia marina*. Ann. Bot. 97, 1095–1101.
Nandy, D.P., Ghose, M., 2005. Photosynthesis and water use characteristics in Indian mangroves. J. Plant Biol. 48, 245–252.
Niu, S., Luo, Y., Fei, S., Yuan, W., Schimel, D., Law, B.E., Ammann, C., Arain, M.A., Arneth, A., Aubinet, M., Barr, A., Beringer, J., Bernhofer, C., Black, T.A., Buchmann, N., Cescatti, A., Chen, J., Davis, K.J., Dellwik, E., Desai, A.R., Etzold, S., Francois, L., Gianelle, D., Gielen, B., Goldstein, A., Groenendijk, M., Gu, L., Hanan, N., Helfter, C., Hirano, T., Hollinger, D.Y., Jones, M.B., Kiely, G., Kolb, T.E., Kutsch, W.L., Lafleur, P., Lawrence, D.M., Li, L., Lindroth, A., Litvak, M., Loustau, D., Lund, M., Marek, M., Martin, T.A., Matteucci, G., Migliavacca, M., Montagnani, L., Moors, E., Munger, J.W., Noormets, A., Oechel, W., Olejnik, J., Paw U, K.T., Pilegaard, K., Rambal, S., Raschi, A., Scott, R.L., Seufert, G., Spano, D., Stoy, P., Sutton, M.A., Varlagin, A., Vesala, T., Weng, E., Wohlfahrt, G., Yang, B., Zhang, Z., Zhou, X., 2012. Thermal optimality of net ecosystem exchange of carbon dioxide and underlying mechanisms. New Phytol. 194 (3), 775–783.
Oren, R., Sperry, J.S., Katul, G.G., Pataki, D.E., Ewers, B.E., Phillips, N., Schäfer, K.V.R., 1999. Survey and synthesis of intra- and interspecific variation in stomatal sensitivity to vapour pressure deficit. Plant Cell Environ. 22, 1515–1526.
Parida, A.K., Das, A.B., Mittra, B., 2004. Effects of salt on growth, ion accumulation, photosynthesis and leaf anatomy of the mangrove, *Bruguiera parviflora*. Trees 18, 167–174.
Patel, N.R., Dadhwal, V.K., Saha, S.K., 2011. Measurement and scaling of carbon dioxide (CO_2) exchanges in wheat using flux-tower and remote sensing. J. Indian Soc. Rem. 39 (3), 383–391.
Rajeevan, M., Unnikrishnan, C.K., Jyoti Bhate, K., Kumar, N., Sreekala, P.P., 2012. Northeast monsoon over India: variability and prediction. Meteorol. Appl. 19, 226–236.
Ravindranath, N.H., Murthy, I.K., 2010. Greening India mission. Curr. Sci. 99, 4.
Reichstein, M., Falge, E., Baldocchi, D., Papale, D., Aubinet, M., Berbigier, P., Bernhofer, C., Buchmann, N., Gilmanov, T., Granier, A., Grünwald, T., Havránková, K., Ilvesniemi, H., Janous, D., Knohl, A., Laurila, T., Lohila, A., Loustau, D., Matteucci, G., Meyers, T., Miglietta, F., Ourcival, J., Pumpanen, J., Rambal, S., Rotenberg, E., Sanz, M., Tenhunen, J., Seufert, G., Vaccari, F., Vesala, T., Yakir, D., Valentini, R., 2005. On the separation of net ecosystem exchange into assimilation and ecosystem respiration: review and improved algorithm. Global Change Biol. 11 (9), 1424–1439.
Reichstein, M., Bahn, M., Ciais, P., Frank, D., Mahecha, M.D., Seneviratne, S.I., Bahn, M., Ciais, P., Frank, D., Mahecha, M.D., Seneviratne, S.I., Zscheischler, J., Beer, C., Buchmann, N., Frank, D.C., Papale, D., Rammig, A., Smith, P., Thonicke, K., Velde, M., Vicca, S., Walz, A., Wattenbach, M., 2013. Climate extremes and the carbon cycle. Nature 500, 287–295.
Robertson, A.I., Alongi, D.M., 2016. Massive turnover rates of fine root detrital carbon in tropical Australian mangroves. Oecologia 180 (3), 841–851.
Rodda, S.R., Thumaty, K.C., Jha, C.S., Dadhwal, V.K., 2016. Seasonal variations of carbon dioxide, water vapor and energy fluxes in tropical Indian mangroves. Forests 7, 35.
Sabbatini, S., Mammarella, I., Arriga, N., Fratini, G., Graf, A., Hörtnagl, L., Ibrom, A., Longdoz, B., Mauder, M., Merbold, L., Metzger, S., Montagnani, L., Pitacco, A., Rebmann, C., Sedlák, P., Šigut, L., Vitale, D., Papale, D., 2018. Eddy covariance raw data processing for CO_2 and energy fluxes calculation at ICOS ecosystem stations. Int. Agrophys. 32, 495–515.
Saintilan, N., Wilson, N.C., Rogers, K., Rajkaran, A., Krauss, K.W., 2014. Mangrove expansion and salt marsh decline at mangrove poleward limits. Global Change Biol. 20 (1), 147–157.
Santini, N.S., Reef, R., Lockington, D.A., Lovelock, C.E., 2015. The use of fresh and saline water sources by the mangrove *Avicennia marina*. Hydrobiologia 745, 59–68.
Sarma, D., Baruah, K.K., Baruah, R., Gogoi, N., Bora, A., Chakraborty, S., Karipot, A., 2018. Carbon dioxide, water vapour and energy fluxes over a semi-evergreen deciduous forest in Assam, Northeast India. J. Earth Syst. Sci. 127 (7), 1–13.
Schmid, H.P., 2002. Footprint modeling for vegetation atmosphere exchange studies: a review and perspective. Agric. For. Meteorol. 113, 159–183.
Selvam, V., 2003. Environmental classification of mangrove wetlands of India. Curr. Sci. 84, 759–765.
Selvam, V., Gnanappazham, L., Navamuniyammal, M., Ravichandran, K.K., Karunagaram, V.M., 2002. Atlas of Mangrove Wetlands of India. M.S. Swaminathan Research Foundation, Chennai, India, pp. 12–58.
Simard, M., Zhang, K., Rivera-Monroy, V.H., Ross, M.S., Ruiz, P.L., Castañeda-Moya, E., Twilley, R.R., Rodriguez, E., 2006. Mapping height and biomass of mangrove forests in Everglades National Park with SRTM elevation data. Photogramm. Eng. Rem. Sens. 72, 299–311.
Simard, M., Fatoyinbo, L., Smetanka1, C., Rivera-Monroy, V.H., Castañeda-Moya, E., Thomas, N., Van der Stocken, T., 2019. Mangrove canopy height globally related to precipitation, temperature and cyclone frequency. Nat. Geosci. 12, 40–45.
Sperry, J.S., Tyree, M.T., Donnelly, J.R., 1988. Vulnerability of xylem to embolism in a mangrove vs inland species of Rhizophoraceae. Physiol. Plantarum 74, 276–283.
Sundareshwar, P.V., Murtugudde, R., Srinivasan, G., Singh, S., Ramesh, K.J., Ramesh, R., Verma, S.B., Agarwal, D., Agarwal, P., Baldocchi, D.D., Baru, C.K., Baruah, K.K., Chowdhury, G.R., Dadhwal, V.K., Dutt, C.B.S., Fuentes, J., Gupta, P.K., Hargrove, M., Howard, W.W., Jha, C.S., Lal, S., Michener, W.K., Mitra, A.P., Morris, J.T., Myneni, R.R., Naja, M., Nemani, R., Purvaja, R., Raha, S., Santhana Vanan, S.K., Sharma, M., Subramaniam, A., Sukumar, R., Twilley, R.R., Zimmerman, P.R., 2007. Environmental monitoring network for India. Science 316 (5822), 204–205.
Takemura, T., Hanagata, N., Sugihara, K., Baba, S., Karube, I., Dubinsky, Z., 2000. Physiological and biochemical responses to salt stress in the mangrove. *Bruguierra gymnorrhiza*. Aquat. Bot. 68, 15–28.
Tan, Z.H., Zhang, Y., Schaefer, D., Yu, G.R., Liang, N., Song, Q.H., 2011. An old-growth subtropical Asian evergreen forest as a large carbon sink. Atmos. Environ. 45, 1548–1554.
Thomas, M.V., Malhi, Y., Fenn, K.M., Fisher, J.B., Morecroft, M.D., Lloyd, C.R., Taylor, M.E., McNeil, D.D., 2011. Carbon dioxide fluxes over an ancient broadleaved deciduous woodland in southern England. Biogeosciences 8, 1595–1613.
Verma, S.B., Baldocchi, D.D., Anderson, D.E., Matt, D.R., Clement, R.J., 1986. Eddy fluxes of CO_2, water vapor, and sensible heat over a deciduous forest. Bound. Lay. Meteorol. 36 (1–2), 71–91.
Walsh, B., Ciais, P., Janssens, I.A., Pen˜uelas, J., Riahi, K., Rydzak, F., Vuuren, D., Obersteiner, M., 2017. Pathways for balancing CO2emissions and sinks. Nat. Commun. 8, 14856.
Wang, W., Liao, Y., Wen, X., Guo, Q., 2013. Dynamics of CO_2 fluxes and environmental responses in the rain-fed winter wheat ecosystem of the Loess Plateau, China. Sci. Total Environ. 461–462, 10–18.
Ward, G.A., Smith, T.J., Whelan, K.R.T., Doyle, T.W., 2006. Regional processes in mangrove ecosystems: spatial scaling relationships, biomass, and turnover rates following catastrophic disturbance. Hydrobiologia 569, 517–527.
Watham, T., Kushwaha, S., Patel, N., Dadhwal, V., 2014. Monitoring of carbon dioxide and water vapour exchange over a young mixed forest plantation using eddy covariance technique. Curr. Sci. 107, 857–867.
Watham, T., Patel, N.R., Kushwaha, S.P.S., Dadhwal, V.K., Senthil Kumar, A., 2017. Evaluation of remote-sensing-based models of gross primary productivity over

Indian sal forest using flux tower and MODIS satellite data. Int. J. Rem. Sens. 38 (18), 5069–5090.
Webb, E.K., Pearman, G.I., Leuning, R., 1980. Correction of flux measurements for density effects due to heat and water vapour transfer. Q. J. R. Meteorol. Soc. 106, 85–100.
Wilczak, J.M., Oncley, S.P., Stage, S.A., 2001. Sonic anemometer tilt correction algorithms. Bound. Lay. Meteorol. 99, 127–150.
Wutzler, T., Lucas-Moffat, A., Migliavacca, M., Knauer, J., Sickel, K., Šigut, L., Menzer, O., Reichstein, M., 2018. Basic and extensible post-processing of eddy covariance flux data with REddyProc. Biogeosciences 15, 5015–5030.
Yu, G.R., Wen, X.F., Sun, X.M., Tanner, B.D., Lee, X.H., Chen, J.Y., 2006. Overview of China FLUX and evaluation of its eddy covariance measurement. Agric. For. Meteorol. 137, 125–137.
Yu, G.R., Zhang, L., Minsun, X., Lingfu, Y., Fawen, X., Wang, F., Li, S., Ren, C., Song, X., Liu, Y., Han, S., Yan, J., 2008. Environmental controls over carbon exchange of three forest ecosystems in eastern China. Global Change Biol. 14 (11), 2555–2571.
Zhu, Z., Sun, X., Wen, X., Zhou, Y., Tian, J., Yuan, G., 2006. Study on the processing method of nighttime CO_2 eddy covariance flux data in China FLUX. Sci. China Earth Sci. 49, 36–46.